Hyd
Eng
Geol

SANDIA REPORT

SAND86—0090 • UC—814
Unlimited Release
Printed April 1990

Yucca Mountain Project

The Thermal Conductivity of the Topopah Spring Member at Yucca Mountain, Nevada

Francis B. Nimick

Prepared by
Sandia National Laboratories
Albuquerque, New Mexico 87185 and Livermore, California 94550
for the United States Department of Energy
under Contract DE-AC04-76DP00789

"Prepared by Yucca Mountain Project (YMP) participants as part of the Civilian Radioactive Waste Management Program (CRWM). The YMP is managed by the Yucca Mountain Project Office of the U.S. Department of Energy, Nevada Operations Office (DOE/NV). YMP work is sponsored by the Office of Geologic Repositories (OGR) of the DOE Office of Civilian Radioactive Waste Management (OCRWM)."

Issued by Sandia National Laboratories, operated for the United States Department of Energy by Sandia Corporation.

Printed in the United States of America. This report has been reproduced directly from the best available copy.

Available to DOE and DOE contractors from
Office of Scientific and Technical Information
PO Box 62
Oak Ridge, TN 37831

Prices available from (615) 576-8401, FTS 626-8401

Available to the public from
National Technical Information Service
US Department of Commerce
5285 Port Royal Rd
Springfield, VA 22161

NTIS price codes
Printed copy: 04
Microfiche copy: A01

SAND86-0090
Unlimited Release
Printed April 1990

Distribution
Category UC-814

THE THERMAL CONDUCTIVITY OF THE TOPOPAH SPRING MEMBER AT YUCCA MOUNTAIN, NEVADA

Francis B. Nimick
Geotechnical Projects Division
Sandia National Laboratories
Albuquerque, NM 87185

ABSTRACT

Measured thermal-conductivity data are summarized for 15 samples of the Topopah Spring Member from Yucca Mountain. Modeling results for the saturation history of thermal-conductivity-experiment samples are presented; the saturation of these samples may be 0.5 or greater even after an experiment is completed. Thus, only the data from low-temperature measurements have been used to obtain estimates of matrix thermal conductivities and then of in situ (rock mass) values for thermal conductivity. The estimated in situ values for Units TSw1 and TSw2 are consistent with experiment data obtained by other investigators.

This report was prepared for a QA Level III Task under WBS 1.2.4.2.1.3.S. The data used in the analyses in the report all have a QA Level of TBD (to be determined) because they were collected before formal institution of the system of QA Levels.

CONTENTS

FIGURES

TABLES

1.0 INTRODUCTION

Yucca Mountain, located in and near the southwest corner of the Nevada Test Site (NTS) in southern Nye County, Nevada (Figure 1), has been identified by the Department of Energy (DOE) as a potential site for the disposal of radioactive waste. Responsibility for studying the suitability of Yucca Mountain as a disposal site rests with the Yucca Mountain Project (YMP), administered by the DOE offices in Las Vegas, Nevada. Sandia National Laboratories (SNL) is one of the primary YMP participants and has responsibilities for performance assessment, repository design, and the measurement of the thermal and mechanical properties of some of the tuff units from Yucca Mountain.

Figure 2 is a summary of the younger stratigraphic units present at Yucca Mountain. All of the units shown in Figure 2 are tuffaceous, but the lithologies vary from bedded, reworked tuffs through nonwelded vitric or zeolitized ash-flow tuffs to densely welded devitrified or vitric ash flows. The Topopah Spring Member of the Paintbrush Tuff (the proposed horizon for waste emplacement) is largely composed of densely welded, devitrified ash flows, the mineralogy of which is predominantly feldspar (plagioclase and alkali feldspar) and silica minerals (quartz, cristobalite, and tridymite).

One set of rock properties to be measured includes those involved in heat transfer. Thermal conductivity is one of the heat transfer properties for which a number of measurements have been made. Experiment results have been presented in a summary of data obtained for all tuff

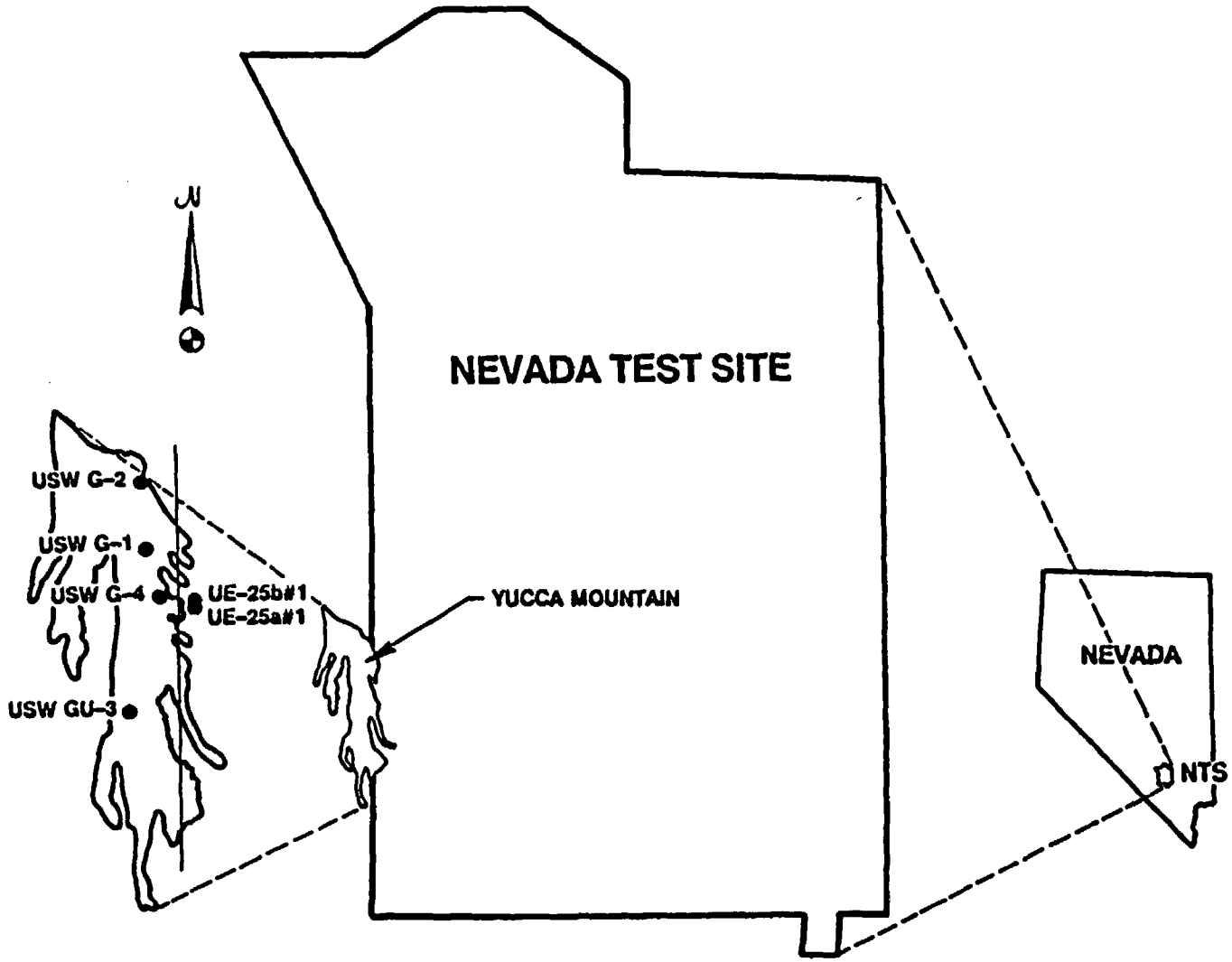

Figure 1. Locations of the Nevada Test Site, Yucca Mountain, and Existing Deep Core Holes.

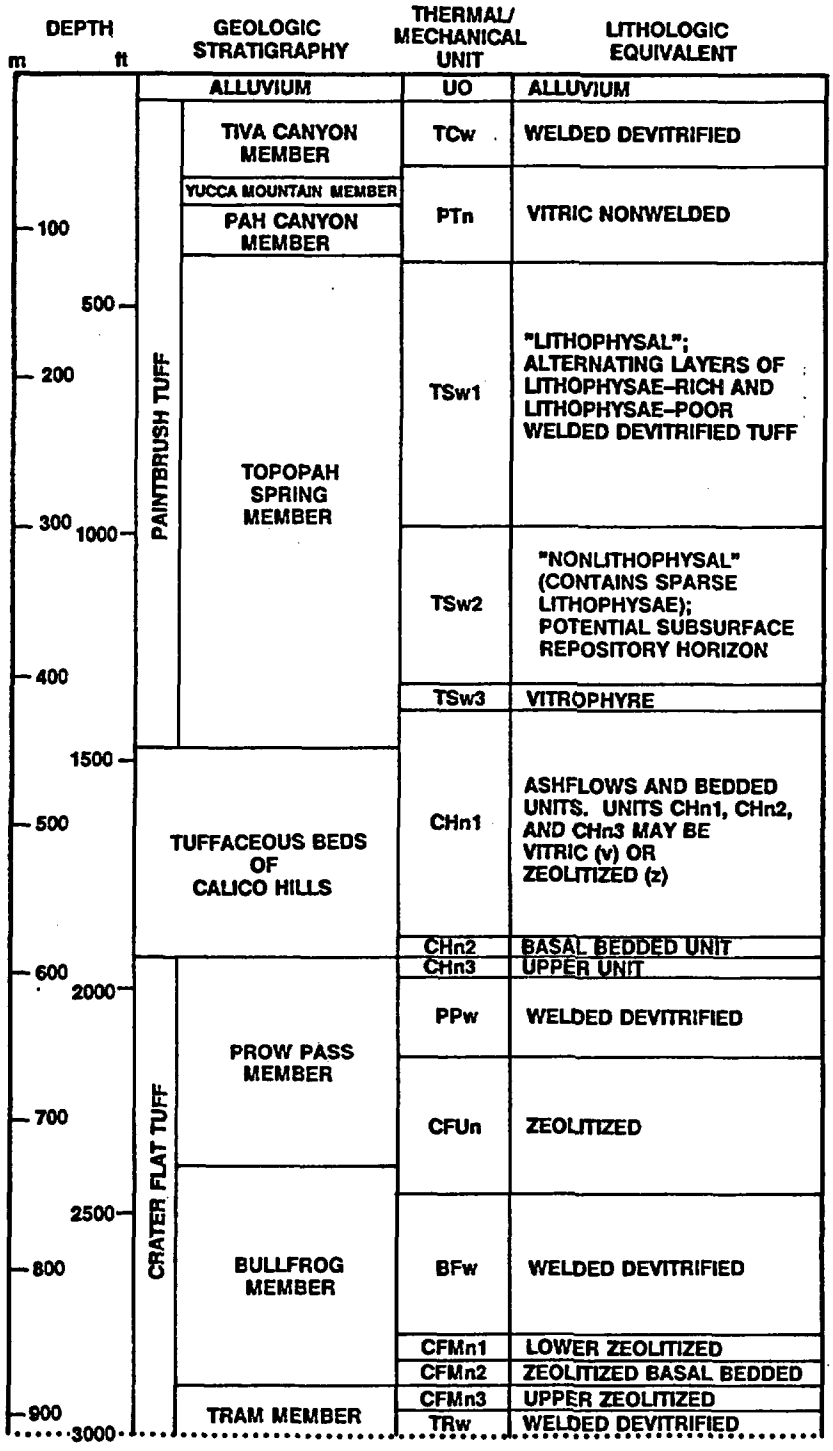

Figure 2. Stratigraphy of Tuffaceous Units at Yucca Mountain. Thicknesses of Units are Averages for the Core Holes Shown in Figure 1.

units at Yucca Mountain (Nimick and Lappin, 1985); a revised set of data for units above the static water level is presented in Nimick (1989). Data for the welded, devitrified portion of the Topopah Spring Member are the basis for analysis in this report.

Calculation of the temperatures to be expected in the Topopah Spring Member as a result of the presence of heat-producing waste requires that the thermal conductivity of the rock be known or approximated. Difficulties arise in the transfer of laboratory-measured thermal-conductivity data to in situ conditions because of differences in the states of saturation. Laboratory samples have been tested either "saturated" or "dry" (the significance of the quotation marks is discussed in more detail later in this report), whereas the in situ thermal conductivity must be known for conditions of partial saturation.

To date, the following sequence of steps has been followed to obtain an estimate of the in situ thermal conductivity (e.g., Nimick and Lappin, 1985):

(1) Measure the "saturated" ($K_{m,s}$) and "dry" ($K_{m,d}$) thermal conductivities of a number of samples of porous matrix material in laboratory tests.

(2) Calculate matrix (zero-porosity) thermal conductivities (K_o) for the "saturated" and "dry" conditions, using a rearranged form of the geometric mean equation (Woodside and Messmer, 1961):

$$K_{o,s} = \frac{K_{m,s}}{K_w^{\phi}}^{\frac{1}{1-\phi}} \tag{1}$$

or

$$K_{o,d} = \frac{K_{m,d}}{K_a^{\phi}}^{\frac{1}{1-\phi}} \tag{2}$$

where K_w is the thermal conductivity of water, K_a is the thermal conductivity of air, and ϕ is the porosity in volume fraction.

(3) Use $K_{o,s}$ to calculate the in situ thermal conductivity below the boiling temperature (T_b) and $K_{o,d}$ to calculate the conductivity above T_b, using the following equations:

$$K_{in\ situ} = K_{o,s}^{(1-\phi)}\ K_w^{\phi s}\ K_a^{\phi(1-s)} \qquad (T<T_b) \tag{3}$$

or

$$K_{in\ situ} = K_{o,d}^{(1-\phi)}\ K_a^{\phi} \qquad (T>T_b) \tag{4}$$

where s is the in situ saturation.

Results of neutron probe measurements in the vicinity of in situ heater tests in G-Tunnel (Zimmerman et al., 1986a, 1986b) support two preliminary conclusions:

(1) pore water in welded tuff does not uniformly vaporize and leave the rock at the normal boiling temperature (T_b), and

(2) even when the rock temperature exceeds T_b for extended periods of time, the rock may retain a residual saturation.

These conclusions suggest at least the possibility that similar pore-water behavior might have occurred during thermal-conductivity experiments in the laboratory. If so, then thermal conductivities measured on "dry" samples are actually representative of material with an unknown level of partial saturation.

The possibility that erroneous assumptions may have been made during the derivation of $K_{o,s}$ and $K_{o,d}$ is even more extensive than indicated in the preceding paragraphs. At temperatures below the boiling temperature, samples have been assumed to be saturated (i.e., all of the void spaces are filled with water). However, experimental data on different saturation techniques indicate that vacuum saturation (the technique most commonly used for the thermal conductivity samples) probably achieves an average saturation value no higher than 0.95 in welded tuff (Nimick and Schwartz, 1987). For earlier thermal conductivity experiments in which samples were only immersed in water before testing, saturations at the initiation of testing were probably even lower. For immersion times of a week (168 hr) to a month (730 hr), a saturation of approximately 0.75 appears to be reasonable for welded tuff (Nimick and Schwartz, 1987). Thus, there is very little reason to expect that thermal-conductivity samples from the welded, devitrified portion of the Topopah Spring Member had initial saturations of 1.0.

To determine whether previously published analyses of thermal conductivity data (Lappin, 1980; Lappin et al., 1982; Lappin and Nimick, 1985a,b; Nimick and Lappin, 1985) are in error, saturation behavior during the thermal-conductivity experiments was modeled using the computer code PETROS (Hadley, 1985). PETROS is a one-dimensional, finite-difference code that computes the transport of water, water vapor, an inert gas (air), and heat through a partially saturated, porous medium. Gas transport includes the effects of Knudsen and binary diffusion plus Darcy flow of the gas mixture.

The results of calculations of the saturation behavior of samples during thermal-conductivity experiments are presented in Section 2.0. The calculations of matrix thermal conductivity of the Topopah Spring Member and estimates of in situ thermal conductivity are discussed in Section 3.0.

2.0 SATURATION BEHAVIOR OF TEST SAMPLES

All of the thermal conductivity measurements on samples of the welded, devitrified Topopah Spring Member have been made using the transient-line-source technique on cylindrical samples (radius of 2.54 cm) with a thermal probe (heater) inserted in an axial hole (heater radius is appproximately 0.16 cm). Samples were jacketed to isolate them from surrounding hydraulic fluid. A schematic of the sample configuration is shown in Figure 3.

The general sequence of steps for testing of each sample was as follows:

1. Application of confining pressure, then pore pressure, at ambient temperature;

2. Application of power to thermal probe for 2 minutes or less;

3. Power turned off and temperature allowed to re-equilibrate at orignial level;

4. Repeat of Step 2;

5. Temperature of system raised to new test temperature and allowed to stabilize; and

6. Repeat of Steps 2 through 5.

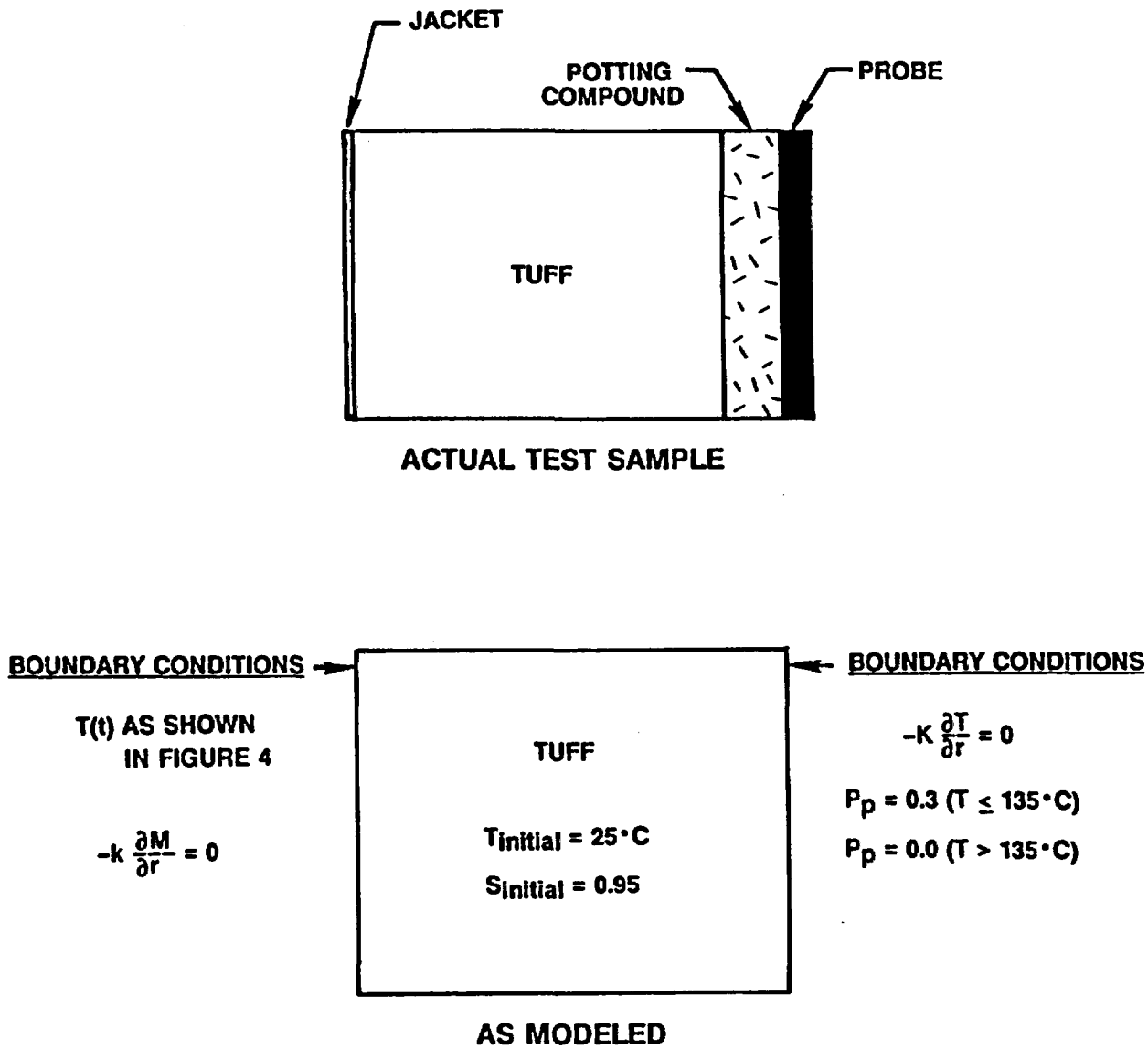

Figure 3. Schematic of Thermal-Conductivity Sample (Actual and As-Modeled).

During each series of measurements, one of the temperature increases (Step 5) crossed through the nominal boiling temperature (at the applied pore pressure) of the pore water. When this temperature was reached, the pore pressure was released, allowing the pore water to "flash" to steam. In theory, all of the pore water would then have been removed from the sample. Part of the reason for the modeling described in the following pages was to determine whether all of the pore water leaves the sample at the boiling temperature.

2.1 Model Input

As input, PETROS requires the geometry of the problem, the initial and boundary conditions for saturation and temperature, and a definition of material properties (e.g., porosity, heat capacity, thermal conductivity, permeability, etc.). Assumptions made to model a thermal-conductivity experiment are described in the following subsections.

2.1.1 Geometry

Actual sample dimensions were assumed. Samples are right circular cylinders with radius of 2.54 cm, each containing a hole of radius 0.5 cm along the axis of the sample. In the model, the hole was assumed to have a radius of 0.16 cm (the radius of the probe); in testing, the gap between the probe and the rock was filled with a potting compound with a high thermal conductivity. Because of the low permeability of the materials and because negligible temperature gradients existed along the axis or around the circumference of a sample, heat and mass transfer can be assumed to be one-dimensional in a radial direction (the assumption of unidimensionality is necessary to use PETROS).

2.1.2 Initial Conditions

The sample was assumed to be at ambient temperature (25°C) at the beginning of a test. The initial saturation was assumed to be 0.95; the effect of assuming a lower initial saturation value is discussed later.

2.1.3 Boundary Conditions

Two types of boundary conditions must be specified--one set governing heat flux (or temperature), and the other type governing mass flux (or saturation). Because of symmetry, the temperature boundary condition at the center of the sample was taken to be one of zero heat flux. At the external boundary, a temperature-time history approximating those actually experienced by thermal-conductivity samples was modeled as shown in Figure 4. The temperature effects resulting from probe firings were assumed to be relatively insignificant for these calculations. This assumption is justified at least in part by the short time span and the small average temperature increases (approximately 1°C) for each firing.

The saturation boundary condition at the external boundary was assumed to be one of zero flux because of the jacketing of the samples. The internal boundary condition reproduced test conditions; for center-line temperatures below 135°C (T_b for the test conditions), a pore pressure equivalent to the test pore pressure (0.3 MPa) was assumed. When the centerline temperature exceeded 135°C, the saturation at the internal boundary was assumed to be zero. Note that this boundary condition is conservative (in terms of maximizing the flux of pore water) because the thermal probe and associated potting compound are in the

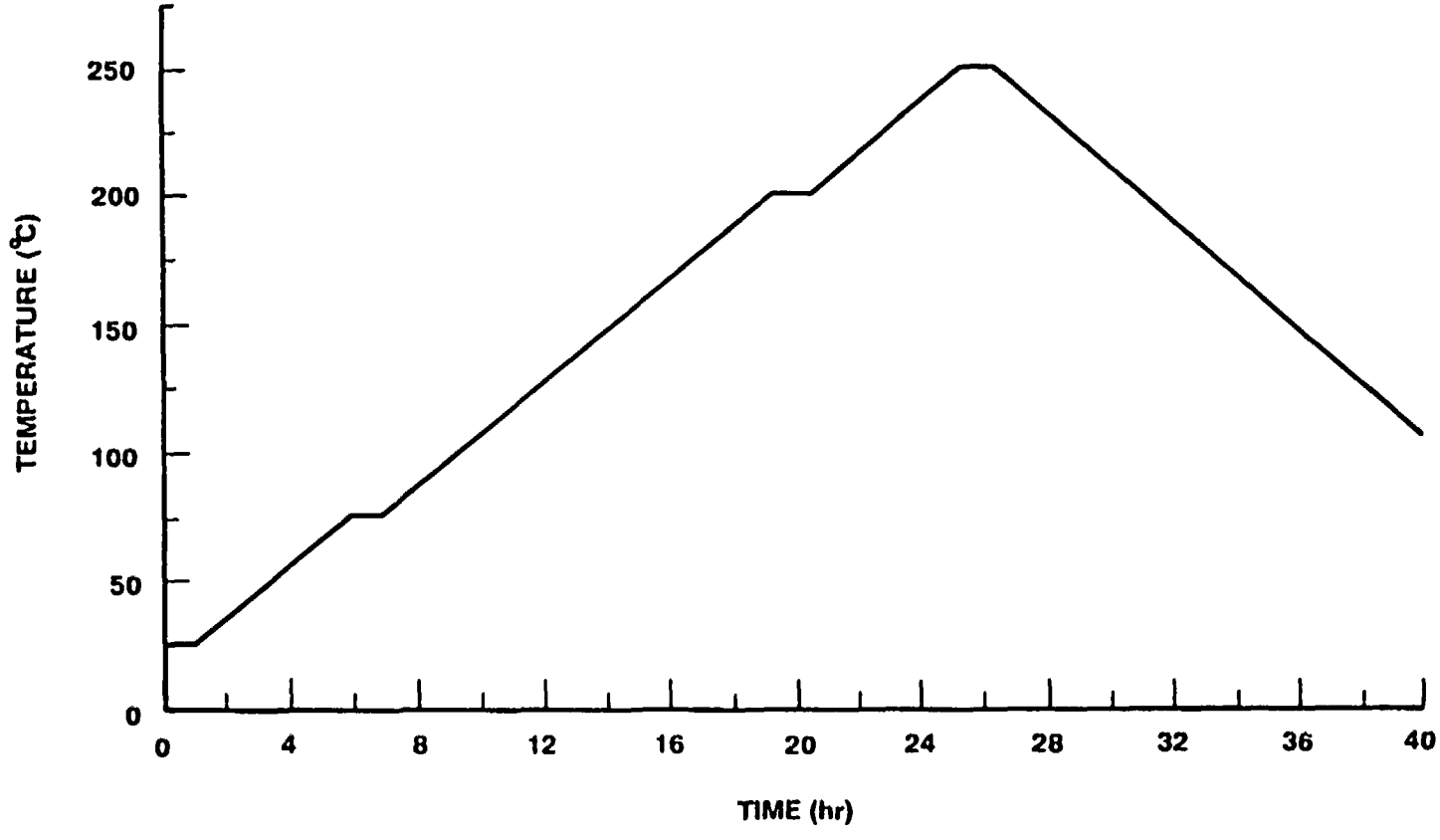

Figure 4. Typical Temperature History of a Thermal-Conductivity Sample (Ignoring Effects of Probe Firings).

central hole during a thermal-conductivity experiment and would impede drying of the sample.

2.1.4 Material Properties

The porosity of test samples of the Topopah Spring Member was assumed to be 0.12, a value close to the average matrix porosity of 0.129 for the welded, devitrified portion of the Member (Nimick and Schwartz, 1987). The heat capacity-density product of the solid is a constant value in PETROS and was assumed to be 2.142 J/cm^3 K [based on a grain density of 2.55 g/cm^3 (Nimick and Schwartz, 1987) and a silicate heat capacity of 0.84 J/g-K (Tillerson and Nimick, 1984, p. 86)]. The thermal conductivity of air (K_a) was assumed for all nonliquid material in pores, and its temperature dependence was taken to be $K_a = (5.39 \times 10^{-5})T + 0.026$,* where T is absolute temperature and K_a is in W/m-K.

The thermal conductivity of water is a very complicated function of pressure and temperature. Rather than using the complete expression of Kestin (1978, p. 47), thermal conductivity as a function of temperature was taken from Table 1 of Kestin (1978, p. 48) at pressures of 0.1 and 0.5 MPa, and an analytical approximation was obtained: $K_w = 0.6988 - 6.284213 \times 10^{13}/T^6$. This equation fits the tabulated data with a correlation coefficient of $r^2 = 0.983$.

---

*Since the modeling was performed, it has been ascertained that this expression is incorrect; 0.026 W/m-K is the value of K_a at ambient temperature rather than 0.042. However, relative to the thermal conductivities of water and rock, the difference is insignificant, and the conclusions drawn from the modeling are still considered to be valid.

The overall thermal conductivity was assumed to be represented by Equation 3 with K_w and K_a as defined above and K_o taken to be 2.43 W/m-K, the average value of $K_{o,s}$ from Nimick and Lappin (1985). The effect of assuming different values for K_o is discussed later.

Hydrologic properties used in the calculations were taken to be representative of the data for the Topopah Spring Member as reported by Peters et al. (1984). The average pore radius was assumed to be 5×10^{-8} m, similar to the values reported by Klavetter and Peters (1987) for the Topopah Spring Member. The pore radius is used by PETROS to calculate the Knudsen diffusion coefficient.

2.2 Results of Calculations

A baseline calculation was performed using the properties specified previously. Following this calculation, four other cases were examined, with different initial and/or boundary conditions:

- K_o = 3.21 W/m-K [maximum value of $K_{o,s}$ from Nimick and Lappin (1985)],
- K_o = 2.15 W/m-K, [minimum value of $K_{o,s}$ from Nimick and Lappin (1985)],
- initial average saturation of 0.75, and
- initial average saturation of 0.75 and internal pore pressure of 0.1 MPa for centerline temperatures less than 100°C.

2.2.1 Results for Baseline Calculation

Output from PETROS includes the temperature and the saturation for each mesh point for each time step for which output is requested. To calculate an average sample saturation, the annular volume represented by each mesh point must be considered. Thus, average saturation (s) is given by

$$s = \frac{1}{V} \sum_{i=1}^{m} s_i V_i \quad , \tag{5}$$

where m is the number of annuli considered, s_i is the calculated saturation of the ith mesh point, V_i is the pore volume at the ith mesh point, and V is the total pore volume of the sample. (Note that for the innermost mesh point, the pore volume is equivalent to the total volume at that point.)

Table 1 and Figures 5 through 9 summarize the results of the baseline calculation. Several conclusions should be highlighted:

(1) Although the initial average saturation is 0.95, the average sample saturation is calculated to be 1.0 after approximately 6 hr, long before the sample temperature reaches T_b.

(2) Figure 8 shows that the sample saturation begins to decrease from 1.0 before T_b is reached. Although this mimics behavior observed in field tests (Zimmerman et al., 1986a, 1986b), the

Table 1

Calculated Temperatures, Average Saturations, and Net Fluxes as a Function of Time for Baseline Calculation

Time (hr)	Temperature (K)	Average Saturation	Net Flux of Pore Water (cm^3)
0	298.0	0.9500	0.000
0.2	298.0	0.9574	0.189
2.9	315.1	0.9956	1.161
6.2	347.8	0.9999	1.269
10.7	383.0	0.9998	1.267
13.3	409.5	0.9655	0.394
13.8	415.6	0.9281	-0.556
15.0	426.6	0.8758	-1.888
16.5	442.3	0.8237	-3.211
18.5	461.7	0.7758	-4.429
20.8	475.0	0.7328	-5.523
22.3	489.6	0.7097	-6.110
24.5	511.7	0.6778	-6.921
26.6	522.6	0.6570	-7.452
27.0	517.3	0.6561	-7.474
29.1	497.8	0.6453	-7.750
32.0	468.6	0.6297	-8.144
34.9	439.5	0.6150	-8.520
37.9	409.7	0.6012	-8.868
41.0	378.9	0.5894	-9.170
44.2	346.8	0.5801	-9.406
47.5	313.6	0.5736	-9.571
56.4	298.0	0.5636	-9.827
182.9	298.0	0.4781	-12.001
287.9	298.0	0.4401	-12.966

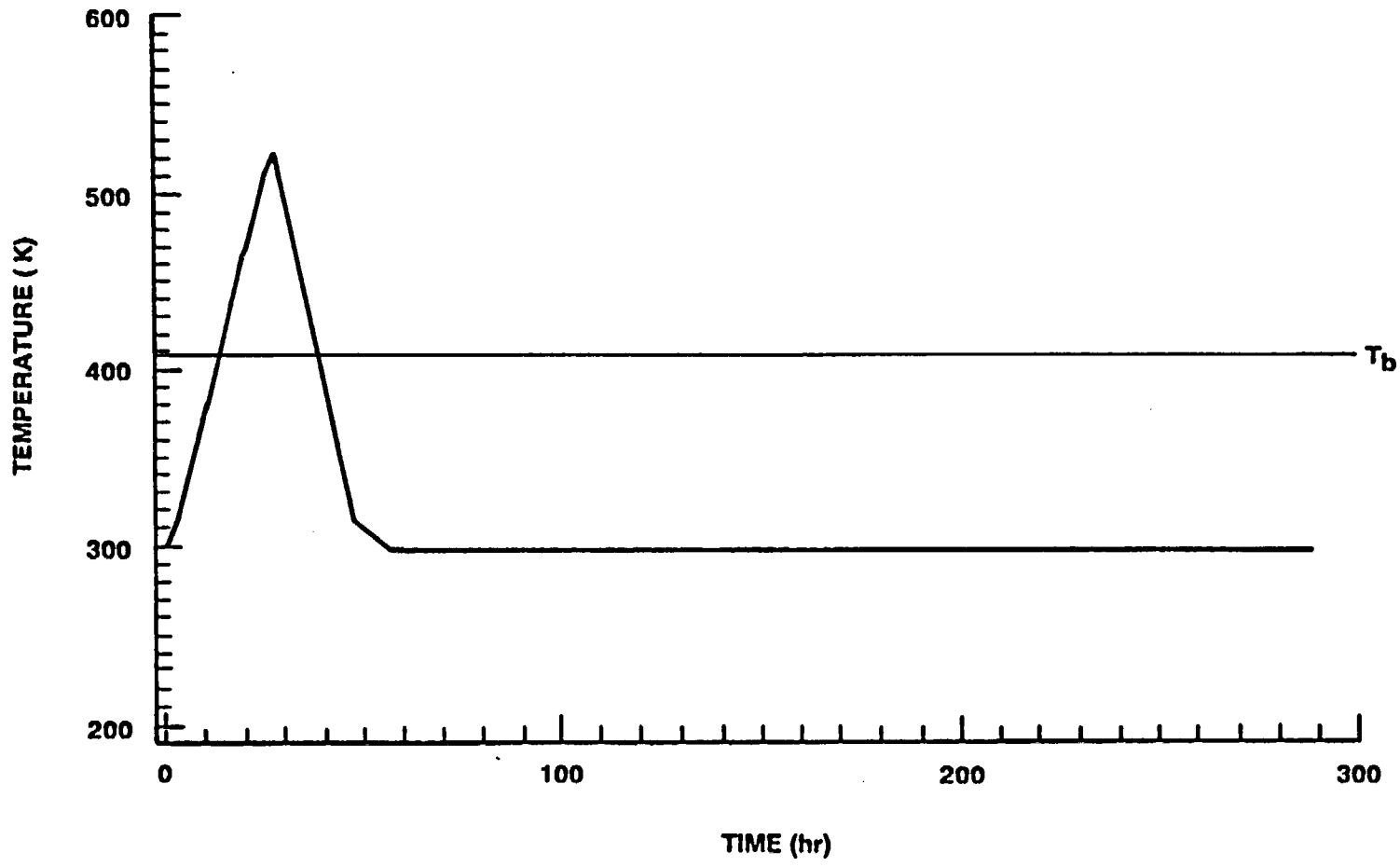

Figure 5. Temperature of a Thermal-Conductivity Sample as a Function of Time.

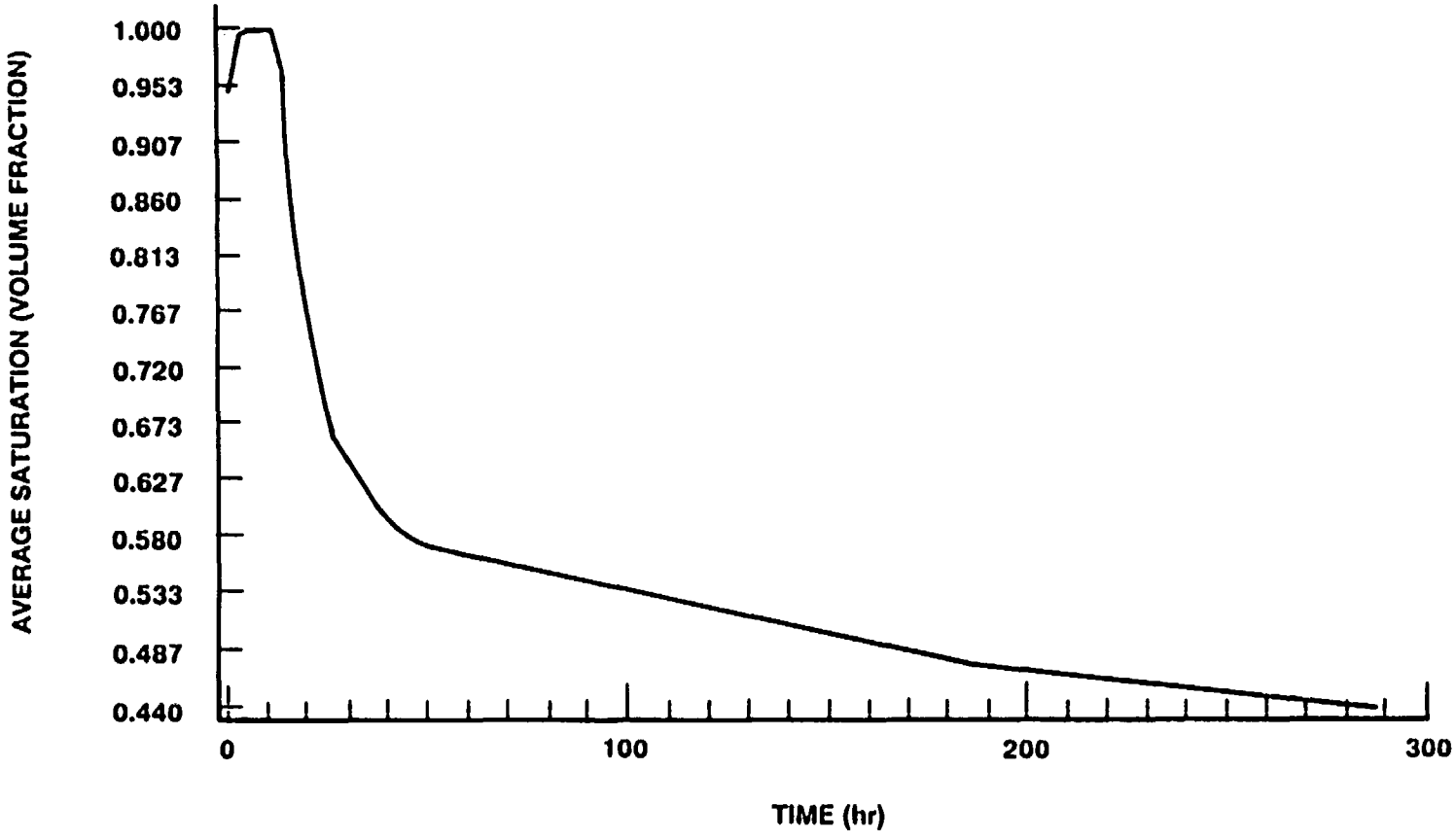

Figure 6. Average Saturation of a Thermal-Conductivity Sample as a Function of Time.

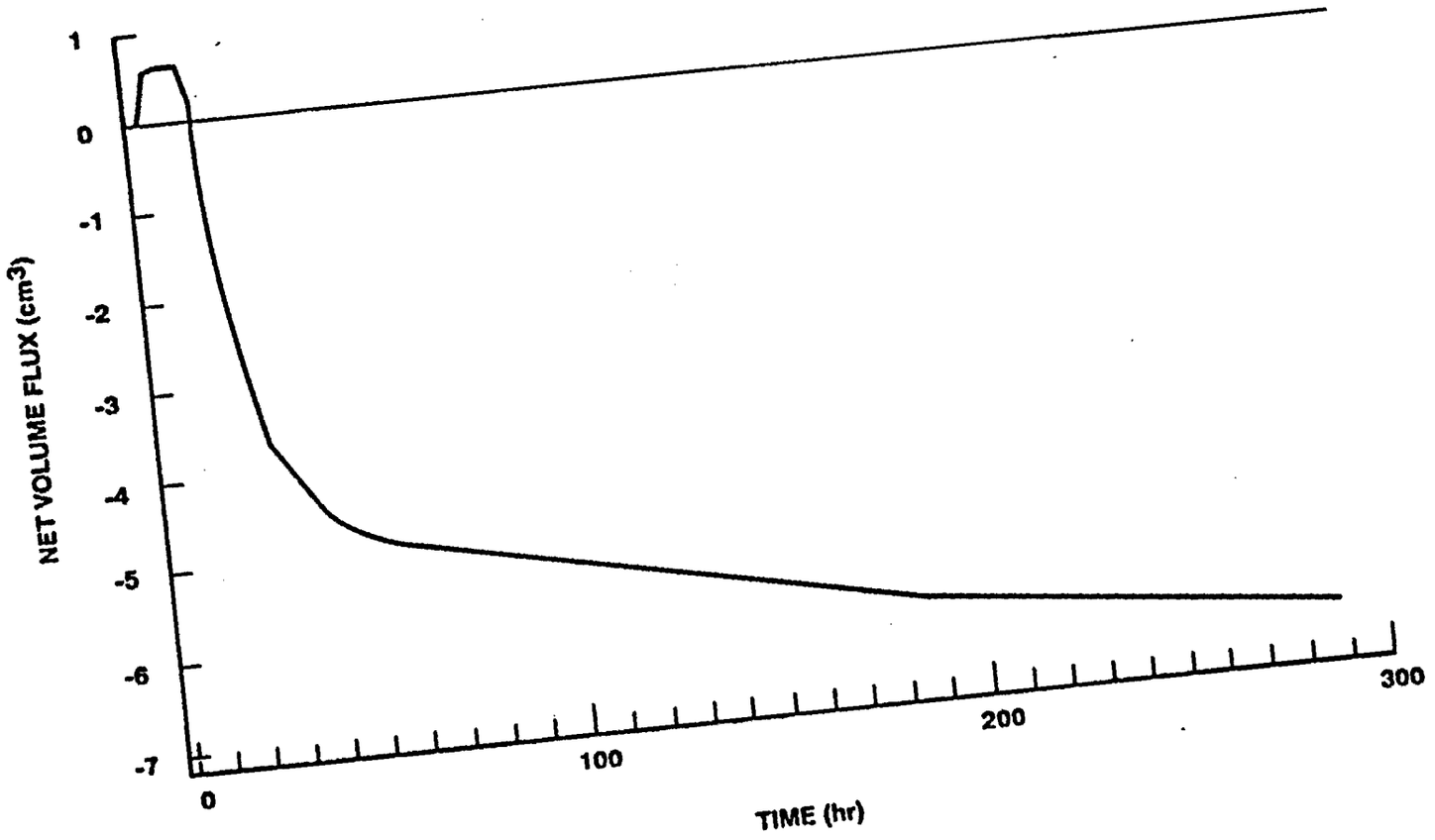

Figure 7. Net Volume Flux of Pore Water as a Function of Time.

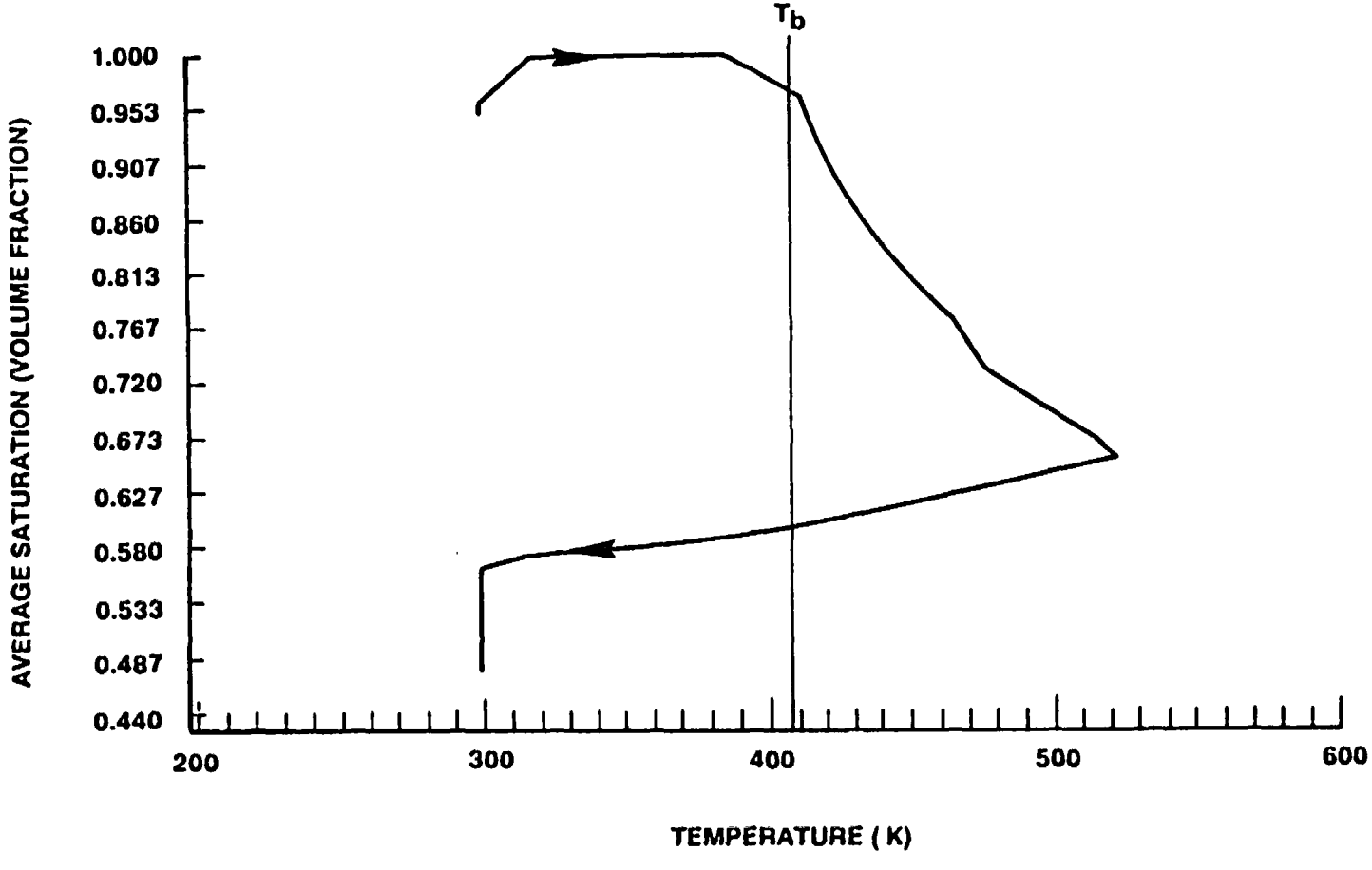

Figure 8. Average Saturation of a Thermal-Conductivity Sample as a Function of Temperature.

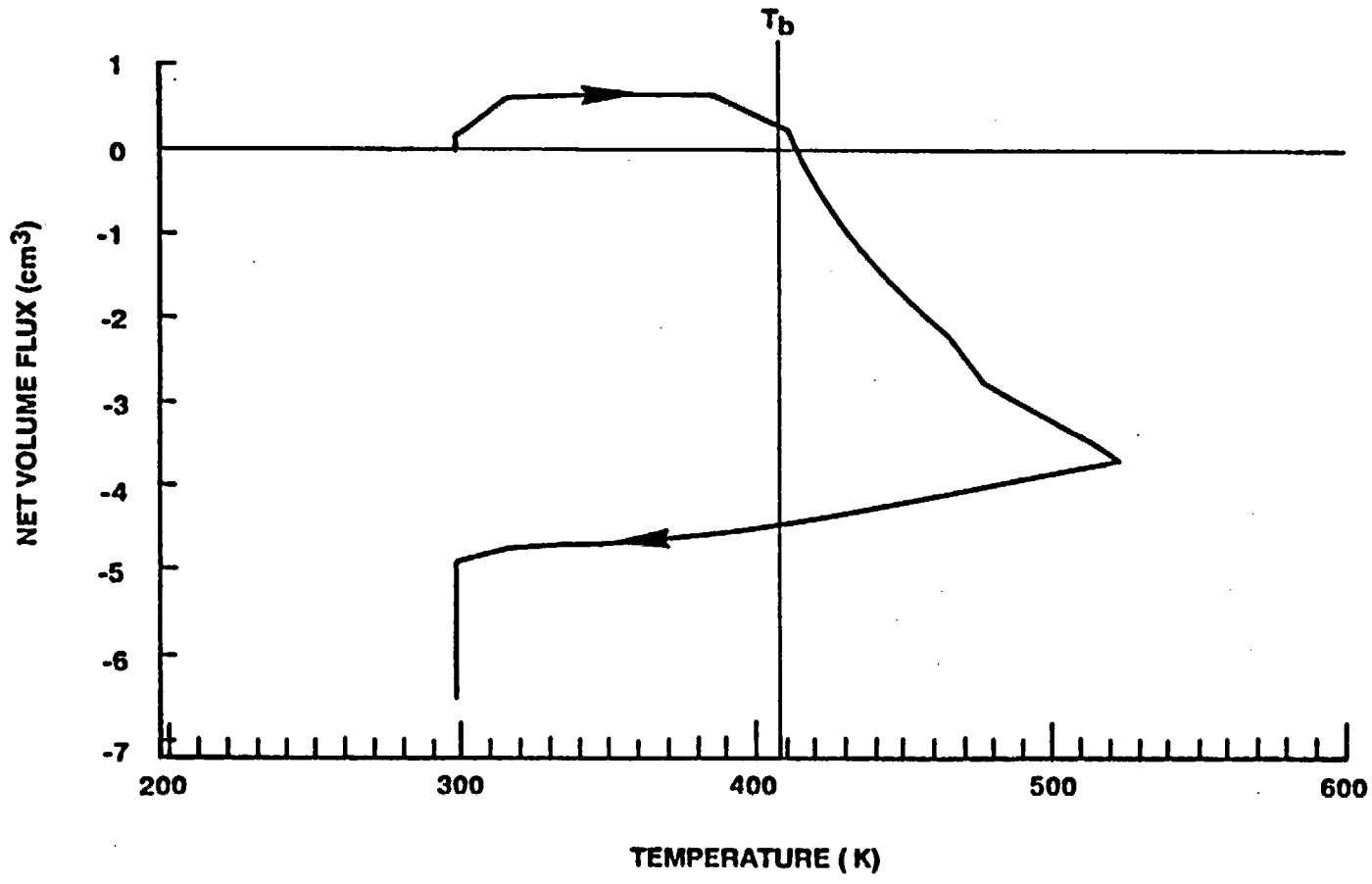

Figure 9. Net Volume Flux of Pore Water as a Function of Temperature.

result for this calculation may occur because the time steps at which data were printed were too far apart.

(3) Figure 8 and Table 1 also indicate that significant average saturations exist in the sample long after the test would be complete (as shown on Figure 4, a test typically takes about 40 hr). Assuming that thermal conductivity measurements were made at 25, 75, 200, 230 and again at 25°C after cooling, average saturations would be approximately 0.95, 1.00, 0.75, 0.68, and 0.56, respectively. Only one of these values--that at 75°C--is equivalent to average saturations assumed in previous data reduction.

(4) Figure 6 shows that allowing the sample to sit at ambient temperature after an experiment with the center hole dry reduces the average sample saturation continuously but at a decreasing rate. Although no conclusion can be reached as to whether a residual saturation would exist, it is clear that the model predicts that very large times would be necessary to completely dry the sample (the last data point has an average saturation of 0.44 after approximately 10 days at ambient temperature).

(5) Figure 7 and Table 1 show the calculated net flex of pore water into or out of the sample as a function of time. At the time at which the sample is calculated to reach ambient temperature after cooling (56.4 hr), the net efflux is calculated to be 9.8 cm^3. This compares to measured volumes of pore fluid

output of 20 to 30 cm^3, a significant discrepancy. In the past, the larger value has been taken to indicate that sample dehydration is essentially complete, because the pore volume in these samples should be approximately 25 cm^3 (for a porosity of 0.12). However, the possibility exists that most of the 20 to 30 cm^3 of water was actually contained in the pore pressure tubing rather than in the sample. This possibility was not checked during the testing and cannot be checked now because the equipment was dismantled in 1986.

(6) Not shown in Figures 5 through 9 or in Table 1 is the result that the thermal conductivity of the sample is sufficiently high that temperature differences across the sample are on the order of 1°C or less. Thus water migration results mainly from pressure gradients rather than from temperature gradients.

2.2.2 Other Calculations

Changing K_o over the expected range of values and performing the same PETROS calculations results in a negligible effect on saturations calculated as a function of temperature or time. The range of values used for K_o corresponds to the minimum and maximum values of $K_{o,s}$ for the Topopah Spring Member calculated at ambient temperature (Nimick and Lappin, 1985).

The combination of an initial saturation of 0.75 with an internal pore pressure of 0.3 MPa affected only the pre-boiling saturation history, as shown in Figure 10. Although the sample requires more time

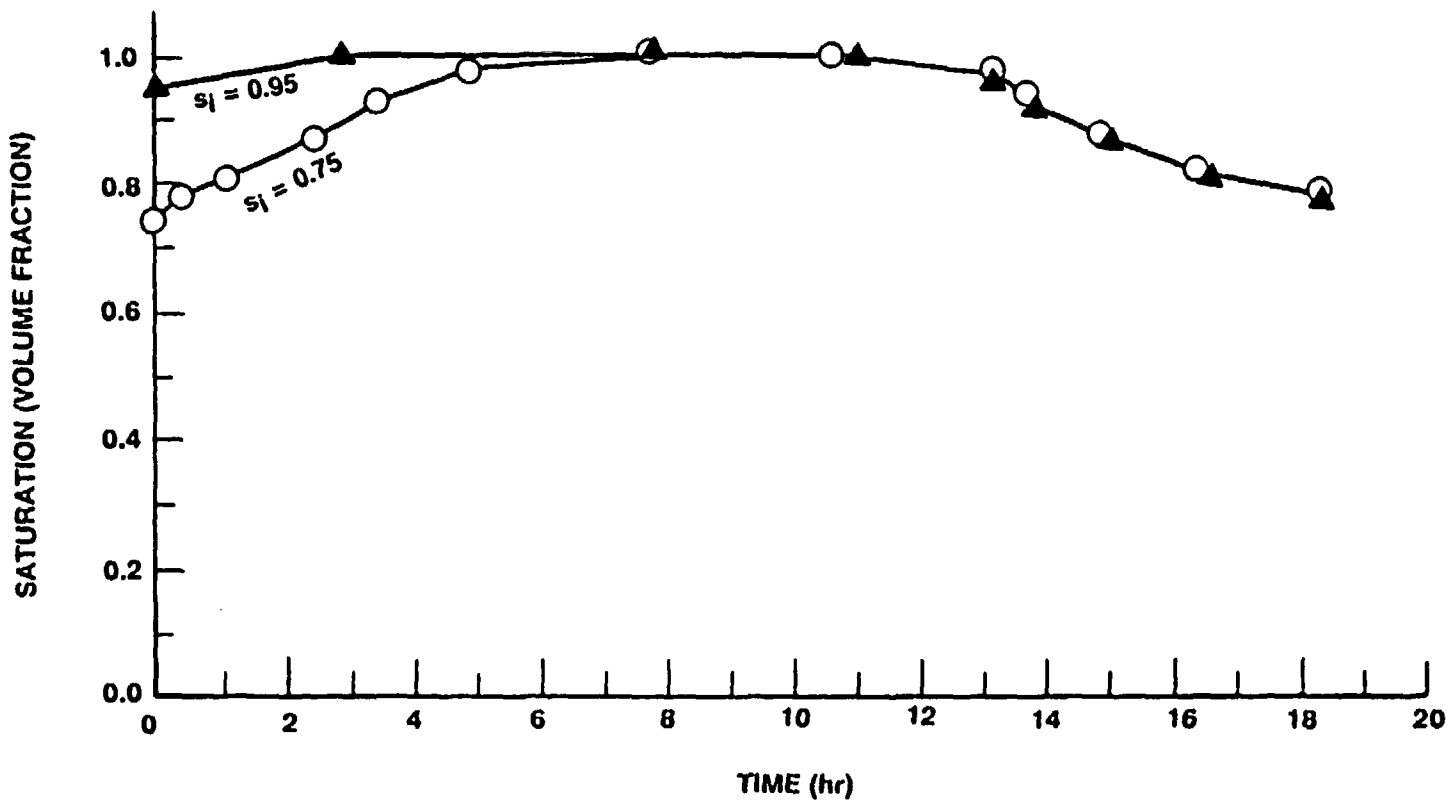

Figure 10. Comparison of Average Saturations as a Function of Time for Two Initial Values for Average Saturation.

to become saturated, saturation is still achieved before boiling occurs (at approximately 12 hr). In fact, the sample temperature at the time that the saturation is greater then 0.999 is only 7°C higher in the case with lower initial saturation.

Calculations using an initial saturation of 0.75 and atmospheric internal pore pressure slowed the saturation process in terms of computation time (i.e., the number of time steps to reach a given total time was greater), so that the arbitrary limit of 300 time steps was reached after only 8.4 hr of a thermal-conductivity experiment had been modeled. However, both the average saturation and the temperature of the sample were equivalent to those for the calculation discussed in the preceding paragraph. Thus, the major difference in tests run without applied pore pressure should be that boiling in the central hole occurs at 95 to 100°C rather than at 135°C. It is assumed that the post-boiling saturation behavior for samples that are not subjected to pore pressure parallels that of the samples tested with pore pressure, with the average saturation at a given temperature taken to be equivalent to that for the samples with pore pressure at a temperature 35°C higher.

2.3 Discussion of Results

Admittedly, there are shortcomings to the analyses performed with PETROS. The effect of temperature on the hydrologic properties, and the possibility that heat transfer, mass transfer, or both are two- or three-dimensional phenomena are two areas in which the validity of the approach cannot be evaluated. Mass transfer probably was at least two-dimensional

during portions of the experiments, because the applied pressure gradient was parallel to the sample axis (see following paragraph), whereas the temperature-induced pressure gradient was perpendicular to the sample axis. However, the axial pressure gradient was applied at temperatures below boiling, and should have been small enough ($\leq$0.3 MPa) that mass transfer was negligible. When temperatures exceeded the nominal boiling temperature, the applied pressure gradient was removed, so that any mass transfer then was solely the result of temperature differences in the sample and the resulting thermal and hydrologic response. Because the temperature distribution should have been a function of radius only (to a first approximation), mass transfer also should have been dominated by radial movement.

Modeling of the boundary conditions for the experiments should have been accurate with one exception. In the model, a hole was assumed to exist in the sample, with a pore pressure applied within the hole for temperatures at or below 135°C and ambient-pressure air in the hole for temperatures above 135°C. In the actual experiments, the central hole contained the thermal probe and a low-permeability potting compound. Thus, the modeling assumpton was not accurate. However, the inaccuracy should have resulted in conservatism in modeling results, in the sense that less water would have left the samples in actual experiments than was modeled to leave. This conclusion is made for two reasons. First, the pore pressure would have been applied at the end of the sample rather than along the axis, so that pore pressures within the sample would have equilibrated more slowly (because of greater distances), and may have been less than 0.3 MPa at the time 100°C was first reached in the sample. Second, once the nominal boiling temperature of 135°C was

reached, water vapor would have had to leave the sample via the interface between the sample and the endcap at one end of the sample, rather than through the axial hole.

The conclusion from the preceding paragraph is that the model should provide an estimate of the maximum amount of water removed from a sample during an experiment. Point 5 of Section 2.2.1 of this report provides a comparison between the modeled amounts of water and the amount of water collected from the sample. This comparison shows a significant discrepancy which is a minimum value because of the conservatism of the model and because only liquid water was collected during the experiment. Any steam leaving the sample would have been collected only if it condensed in the pore-pressure line. Thus, the indications from consideration of the modeling results and the underlying assumptions are tha significant quantities of water may have remained in the samples after experiments were deemed to be complete.

The actual test data (given in Table 2) for "dry" samples lend at least empirical support for the general conclusion that the amount of pore water is continually decreasing throughout the higher-temperature measurements. The data are plotted in Figure 11. Without exception, for samples on which measurements were made at two or more temperatures above T_b, thermal conductivity decreases with increasing temperature. This trend could be caused by decreasing saturation, by a decreasing thermal conductivity in the matrix (i.e., the constituent minerals), or both. Lappin (1980) summarized existing data for the temperature dependence of thermal conductivities of the major minerals in Yucca Mountain tuffs; only quartz showed a decreasing thermal conductivity with increasing

Table 2

Measured Thermal Conductivities as a Function of Temperature

Temperature (°C)	K(W/m-K)	Saturation State[1]
G1-406.4[2]		
25	1.82	S
50	1.82	S
100	1.85	S
165	1.63	D
200	1.62	D
230	1.58	D
G1-795.0		
23	2.14	S
100	2.13	S
165	2.05	S
G1-810.3		
25	2.19	S
50	2.16	S
100	2.15	S
165	2.24	D
200	2.18	D
230	1.95	D
260	1.87	D
G1-1207.9		
50	2.29	S
100	2.29	S
165	2.20	D
200	2.12	D
230	1.99	D
260	1.96	D
G1-1230.8		
25	2.37	S
50	2.36	S
100	2.33	S
G2-860.4		
23	1.88	S
50	1.86	S
100	1.92	S

Table 2 (Continued)

Measured Thermal Conductivities as a Function of Temperature

Temperature (°C)	K(W/m-K)	Saturation State[1]
G2-950.1		
50	2.16	S
100	2.19	S
200	1.87	D
230	1.85	D
260	1.86	D
G2-1272.4		
23	2.11	S
50	2.11	S
100	2.10	S
G2-1388.0		
25	2.24	S
50	2.27	S
100	2.19	S
165	2.24	D
200	1.87	D
230	1.81	D
260	1.79	D
G2-1526.3		
25	1.99	S
G2-1559.0		
25	2.23	S
260	1.99	D
GU3-431.5		
25	1.77	S
235	1.69	D
GU3-683.8		
25	2.15	S
80	2.08	S
200	2.36	D
260	1.76	D

Table 2 (Concluded)

Measured Thermal Conductivities as a Function of Temperature

Temperature (°C)	K(W/m-K)	Saturation State[1]
G4-1155.4		
25	2.48	S
75	2.37	S
200	1.97	D
250	1.88	D
G4-1232.0		
25	2.54	S
75	2.27	S

1: S = saturated; D = "dry."
2: Sample ID is comprised of the core-hole designator (e.g., G1 or G4) and the sample depth in feet.

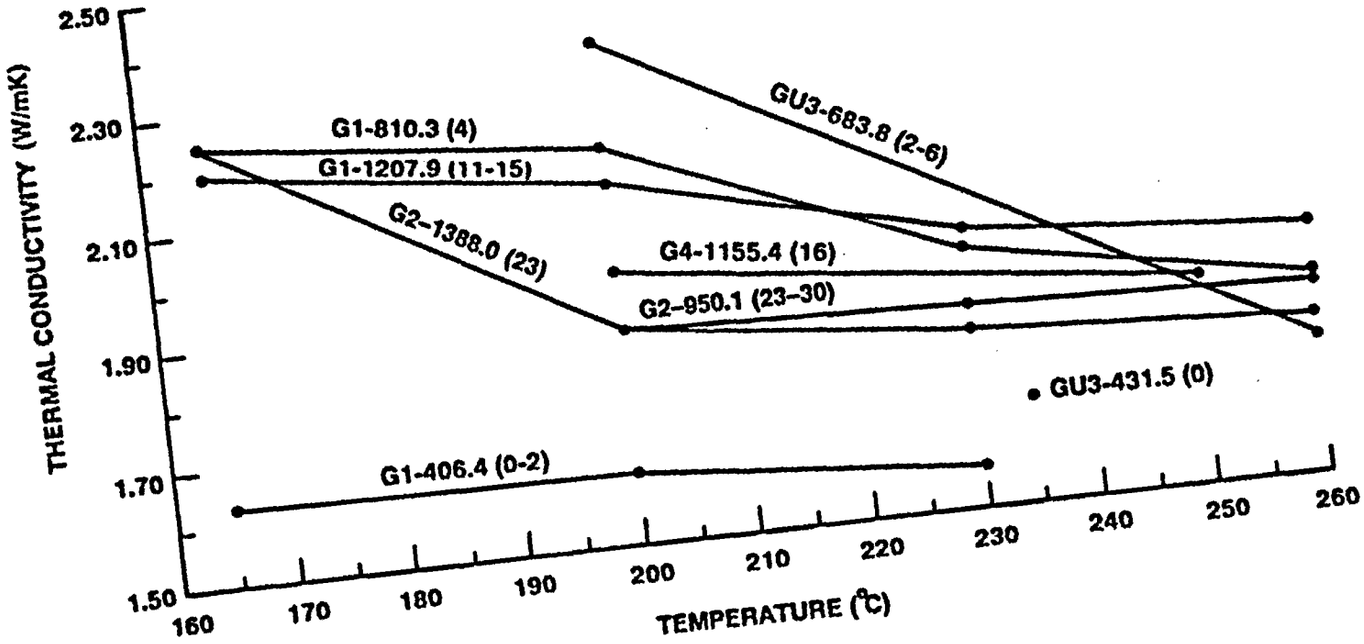

Figure 11. Measured Thermal Conductivity as a Function of Temperature (Above the Nominal Boiling Temperature). Numbers in Parentheses are Quartz Contents (Volume Percent) Estimated From Data in Bish and Chipera (1989).

temperature. Estimation of the quartz contents (data in Bish and Chipera, 1989) of the seven thermal-conductivity samples for which lines are plotted in Figure 11 shows that any correlation between slope of the lines and quartz content is weak to nonexistent. This observation strongly implies that the average saturation of the sample is decreasing as the measurement temperature increases (for temperatures above the nominal boiling temperature).

There are two major implications of this conclusion about average sample saturation. First, the average saturation of thermal-conductivity samples is unknown at any temperature above the boiling temperature. Modeling with PETROS can provide estimates of the average saturation, but the uncertainty in these estimates is probably sufficiently large that calculation of reliable values of $K_{o,d}$ from the measured thermal conductivities is not possible.

Second, and more important, is the implication about the distribution of pore water in the samples at temperatures above the boiling temperature. Figure 12 plots the results of PETROS calculations for this distribution as a function of time. It is clear in this figure that there is a steep gradient in the saturation profile in the central 10% of the sample, with a gradual decrease in the gradient outward until relatively constant values of saturation are attained at approximately 65% of the distance to the sample boundary. Thus, the material cannot be considered to be homogeneous in terms of either saturation or thermal conductivity (the latter would be higher in the outer portions of the sample). The existence of heterogeneity in a sample violates one of the initial

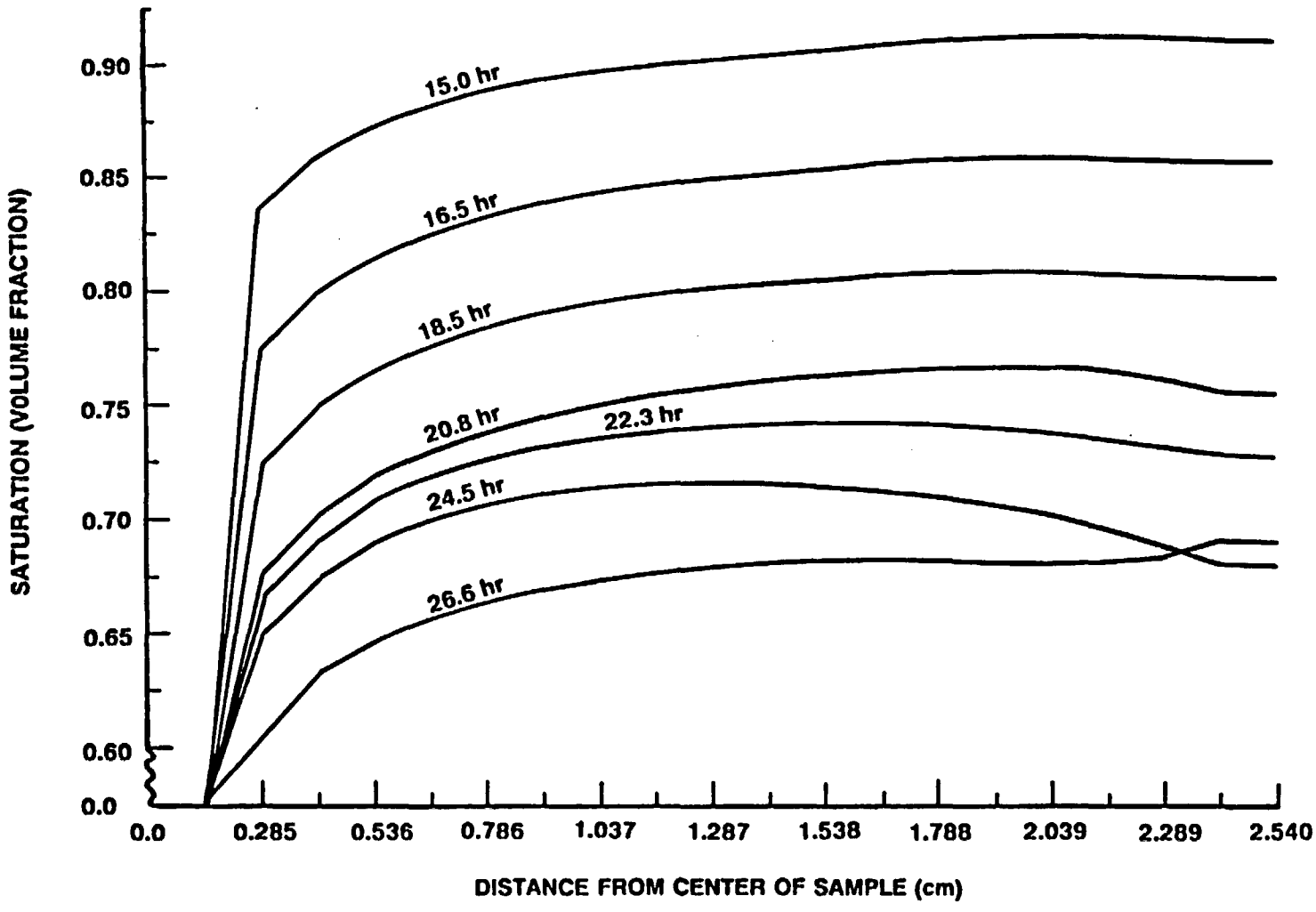

Figure 12. Calculated Saturation as a Function of Radial Position at Various Times During a Thermal-Conductivity Experiment.

assuptions that must be satisfied in order to use the transient-line-source technique: the sample must be composed of material which is homogeneous on the scale of measurement.

The combination of the unknown average saturation of the sample and the heterogeneity of the material during high-temperature measurements results in uncertainty regarding the usefulness of the high-temperature data. Therefore, the decision has been made not to use thermal-conductivity for any analyses that may lead to estimation of in situ thermal conductivity.

3.0 ESTIMATION OF MATRIX AND IN SITU THERMAL CONDUCTIVITIES

The main implications of the results of the calculations using PETROS is that previous analyses of K_o (Lappin, 1980; Lappin et al., 1982; Lappin and Nimick, 1985a,b; Nimick and Lappin, 1985) are incorrect, and that measured thermal-conductivity data at temperatures above the boiling temperature cannot be used to deduce $K_{o,d}$. Therefore, thermal-conductivity data from low-temperature measurements on samples from the welded, devitrified portion of the Topopah Spring Member are the only data reanalyzed in the remainder of this report.

3.1 Estimation of Matrix Thermal Conductivity

The first part of the new analysis is a change in the equation used to calculate $K_{o,s}$ from measured data. The geometric-mean equation (Equations 1 through 4) has been used to interpret all SNL-generated thermal-conductivity data in the past. In general, this method of interpretation has been valid because it was applied predominantly to data from saturated samples and the equation was used both to derive $K_{o,s}$ and to extrapolate $K_{o,s}$ back to in situ thermal conductivities. However, as pointed out by Woodside and Messmer (1961), the geometric-mean equation may not be a good choice when the ratio of the thermal conductivity of the solid to that of the pore fluid is greater than 20. For the tuff samples containing only air in the pores, the ratio would be greater than 50.

Thus a new equation has been selected for use in analyzing the thermal-conductivity data. The equation is one of several proposed by

Brailsford and Major (1964), and is based on a random mixture of two phases. If the two phases are solid and fluid, then the equation is written as follows:

$$K = \frac{1}{4} \; [3(1 - \phi)-1]K_o + (3\phi - 1)K_f \pm$$

$$[3(1 - \phi)-1]K_o + (3\phi - 1)K_f^{\;2} + 8K_oK_f^{\;1/2} \qquad (6)$$

where ϕ is the porosity and K_f is the thermal conductivity of the fluid. Solving for the thermal conductivity of the solid yields

$$K_o = \frac{2K^2 - KK_f(3\phi - 1)}{K(2 - 3\phi) + K_f} \quad . \qquad (7)$$

If a sample is saturated, K_f is the thermal conductivity of water (K_w). If saturation is incomplete, the fluid is treated as a random mixture of air and water; Equation 6 is used to calculate K_f as follows:

$$K_f = \frac{1}{4} \; [3(1 - s)-1] \; K_a + (3s - 1) \; K_w \pm$$

$$[3(1 - s)-1] \; K_a + (3s - 1)K_w^{\;2} + 8K_aK_w^{\;1/2} \qquad (8)$$

where K_a is the thermal conductivity of air.

It is appropriate to compare the values of thermal conductivity predicted by the Brailsford and Major formulation with the values obtained using the geometric-mean equation. Figure 13 shows the two sets of

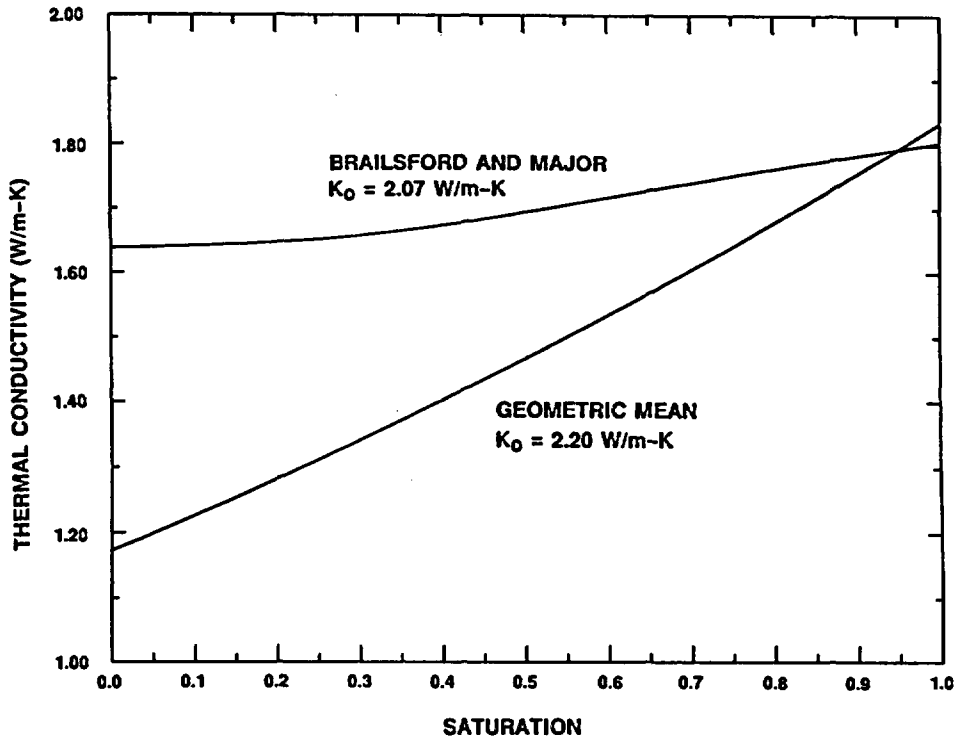

a. Unit TSw1

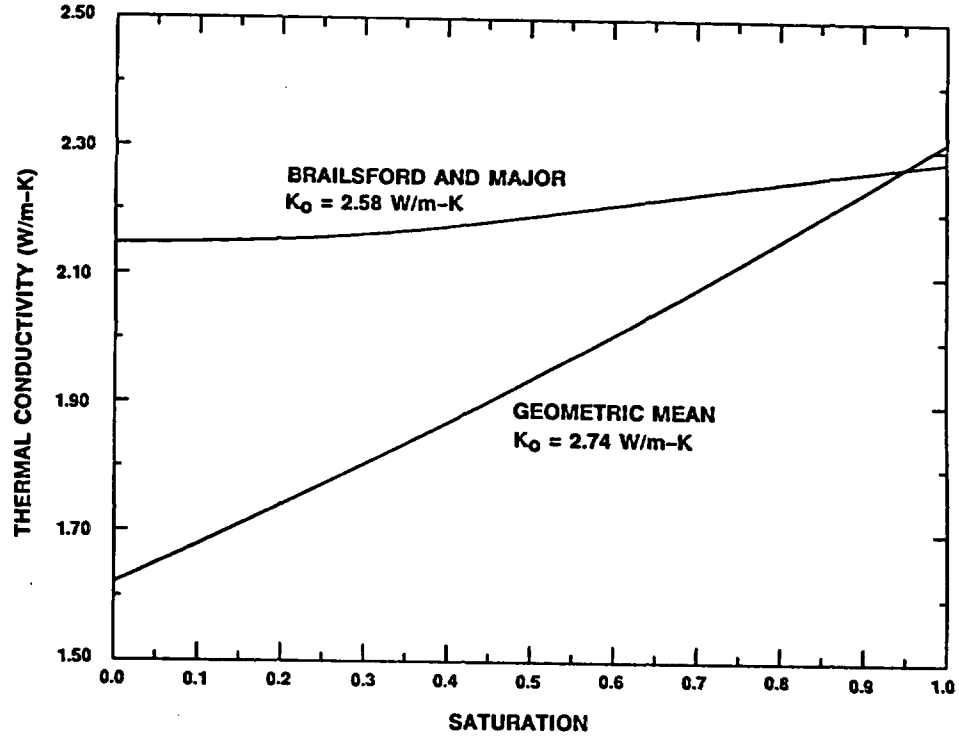

b. Unit TSw2

Figure 13. Calculated Thermal Conductivities of Units TSw1 and TSw2 as a Function of Saturation.

calculated values as a function of saturation for Units TSw1 and TSw2. [The curves in the figure were obtained using mean measured thermal conductivities at 25°C (from data in Table 2), unit-average values for porosity (see following page), and an assumed saturation for the test samples of 0.95.] It is appparent in Figure 13 that the choice of extrapolating equation makes little difference at high saturations, but is more important as the extent of extrapolation increases.

There are two reasons for selection of the Brailsford and Major (BM) equation over the geometric-mean equation. As will be obvious later in the discussion, neither reason can be construed as proof that one equation is better than the other. Instead, the reasons suggest that the BM equation is the better choice.

The first reason is that comparison of Figures 12 and 13 suggests that, at low saturations, the geometric-mean equation estimates thermal conductivities that are substantially lower than expected from experiment results. This is particularly true for Unit TSw1 (Figure 13a). Second, the BM equation was derived based on a physical model of materials, whereas the geometric-mean equation is entirely empirical.

The geometric-mean equation originally was selected by Lappin (1980) for use in tuffs because of ease of computation and successful use of the equation in other rock types. Present selection of the BM equation has been made for somewhat less tenuous reasons; the validity of the selection will need to be verified by obtaining reliable data for samples with low or zero values of saturation.

Table 3 lists the values of s, K_a and K_w used in calculating K_o from the thermal conductivities measured at temperatures at or below 100°C. Values for porosity (ϕ) are not available for individual samples. Rather then attempting to estimate the values, the following steps have been followed:

(1) Calculate a mean value and standard deviation for the measured thermal conductivity (K_m) at each temperature for units TSw1 and TSw2 separately.

(2) Calculate a mean value and standard deviation for K_o using the information from Step 1, the following matrix porosity data from Nimick and Schwartz (1987):

TSw1: $\phi_m = 0.142 \pm 0.038$

TSw2: $\phi_m = 0.113 \pm 0.026$,

and Equations 7 and 8. [The method of propagating uncertainty (e.g., standard deviations) during the calculations is outlined in Appendix A.]

The results of these calculations are given in Table 4.

Statistical comparison (pair-wise t tests) of the mean values in Table 4 indicates that the values of K_o at different temperatures are indistinguishable. Thus, it has been assumed that K_o is independent of temperature, and the mean values given in Table 4 have been averaged (weighted by the number of samples) to give the following values of K_o:

Table 3

Data for Thermal Conductivities of Air and Water and for Average Saturation of Samples

Temperature (°C)	Average Saturation	Thermal Conductivity (W/m-K)	
		Water	Air
23	0.95	0.6054	0.0259
25	0.95	0.6091	0.0261
30	0.97	0.6176	0.0265
50	1.00	0.6435	0.0280
60	1.00	0.6527	0.0288
75	1.00	0.6634	0.0299
80	1.00	0.6663	0.0303
100	1.00	0.6755	0.0317

Table 4

Calculated Matrix Conductivities as a Function of Temperature

Temperature (°C)	Matrix Conductivity (W/m-K) Mean Value	Standard Deviation	n
Unit TSw1			
25	2.07	0.10	2
50	2.24	0.25	3
100	2.28	0.24	3
Unit TSw2			
23	2.40	0.08	2
25	2.58	0.23	8
50	2.52	0.14	5
75	2.61	0.11	2
100	2.46	0.13	6

TSw1: 2.20 ± 0.21 W/m-K (n = 8)

TSw2: 2.51 ± 0.17 W/m-K (n = 23).

The two mean values above are statistically different based on a pair-wise t test.

3.2 Estimation of In Situ (Rock Mass) Thermal Conductivity

The values obtained for the matrix thermal conductivities can be combined with information on matrix porosity, lithophysal-cavity abundance, fracture porosity, and in situ saturation to estimate the in situ thermal conductivities of Units TSw1 and TSw2. The estimation involves several steps. First, the thermal conductivity of the fluid is estimated using Equation 8. (This estimation is the same as that used in the preceding section for the thermal conductivity of the pore fluid in the laboratory samples.) Montazer and Wilson (1984) state that the saturation of the matrix porosity in the Topopah Spring welded unit is 0.65 ± 0.19. The thermal conductivity of the fluid at this saturation level is given Table 5.

The second step is to use these values for K_f, the values of K_o, and Equation 6 to estimate the thermal conductivity of the material without lithophysal cavities or fractures. The results of such an estimation are given in Table 6. Note that it is assumed for the purpose of making these estimations that all pore water is removed at temperatures above 100°C. It is realized that the nominal boiling temperature at Yucca Mountain probably is somewhat lower than 100°C, and that some pore water

Table 5

Thermal Conductivity of Pore Fluid as a Function of Temperature

T (°C)	K_f (W/m-K) Mean Value	K_f (W/m-K) St. Dev.
25	0.3152	0.1538
50	0.3334	0.1623
75	0.3446	0.1666
100	0.3521	0.1689
125	0.0335	NA
150	0.0355	NA
175	0.0370	NA
200	0.0387	NA
225	0.0403	NA
250	0.0419	NA

Table 6

Estimated Thermal Conductivities of Nonlithophysal, Unfractured Material

	Thermal Conductivity (W/m-K)			
	Unit TSw1		Unit TSw2	
Temperature (°C)	Mean Value	St. Dev.	Mean Value	St. Dev.
25	1.84	0.22	2.17	0.17
50	1.84	0.22	2.18	0.17
75	1.85	0.22	2.18	0.17
100	1.85	0.22	2.18	0.17
125	1.75	0.22	2.10	0.18
150	1.75	0.22	2.10	0.18
175	1.75	0.22	2.10	0.18
200	1.75	0.22	2.10	0.18
225	1.76	0.22	2.10	0.18
250	1.76	0.22	2.10	0.18

may be retained to higher temperatures because of local increases in pore pressure. However, the values given in Table 6 are believed to be close to those that will pertain in the majority of cases. This is especially true because of almost total absence of temperature dependence shown by the values in Table 6. Because the estimated thermal conductivities do not appear to be temperature dependent, the data in Table 6 have been combined to give the following values:

	In Situ Saturation	Dry
TSw1	1.85 ± 0.22 W/m-K	1.75 ± 0.22 W/m-K
TSw2	2.18 ± 0.17 W/m-K	2.10 ± 0.18 W/m-K

These values can be combined with data on lithophysal-cavity abundance and fracture porosity to obtain what are perhaps the most relevant estimates of in situ thermal conductivity for units Tsw1 and TSw2. Nimick and Schwartz (1987) provide the following values for lithophysal-cavity abundance (ϕ_{LC}):

TSw1: 0.045 ± 0.061

TSw2: 0.010 ± 0.019

Fracture porosities (ϕ_f) for these two units have been estimated by Klavetter and Peters (1986) to be 4.1×10^{-5} for TSw1 and 18×10^{-5} for TSw2. The fluid in both the lithophysal cavities and the fractures is assumed to be air because the units are partially saturated. Thus, Equation 6 can be used once more, this time with $\phi = \phi_f + \phi_{LC}$. The estimated values are as follows:

	In Situ Saturation	Dry
TSw1	1.73 ± 0.26 W/m-K	1.64 ± 0.26 W/m-K
TSw2	2.14 ± 0.18 W/m-K	2.07 ± 0.18 W/m-K

These are the values that should be used in most thermal calculations involving units TSw1 and TSw2.

Some material in unit TSw1 is distinctly different than the average material because of a higher content of lithophysal cavities. For such material (characteristic of the lower lithophysal zone that is immediately above the TSw1-TSw2 contact), data from Nimick and Schwartz (1987) have been used to estimte a lithophysal-cavity content of 0.095 ± 0.035. Using these values and K_o for unit TSw1, the following thermal conductivities are estimated for material with a high lithophysal-cavity content:

In Situ Saturation: 1.59 ± 0.21 W/m-K

Dry: 1.51 ± 0.21 W/m-K

3.3 Comparison With Other Data

Sass et al. (1988) report numerous thermal-conductivity values for samples which have been assumed to have retained in situ saturations. These data have not been used in estimating in situ thermal conductivities because procedures for coring and sample handling contribute to uncertainty about the comparability of the sample saturations and true in situ saturations. However, the data in Sass et al. (1988) for samples from Units TSw1 (n = 8) and TSw2 (n = 19) allows a check on the

reasonableness of the values estimated in this report. The comparable thermal conductivities are given below.

	This Report	Sass et al.
TSw1	1.73 ± 0.26	1.79 ± 0.27
TSw2	2.15 ± 0.18	2.05 ± 0.18

Statistical comparisons (pair-wise t tests) indicate that the two mean values for each unit cannot be differentiated. Clearly, the data for in situ thermal conductivity obtained by the two different paths are consistent.

3.4 Representativeness of Results

The thermal conductivity of a rock sample is a function of the thermal conductivities of the constituents of the sample and the volume fractions of the constituents. For Units TSw1 and TSw2, the major constituents are alkali feldspar, quartz, cristobalite, and tridymite in the solid portion (Bish and Chipera, 1989) and water and air in the pores. For this report, unit-wide averages have been used for porosity and saturation, so fluid effects on estimated thermal conductivity should be uniform and representative. In addition, the 11 samples from Unit TSw2 are from various stratigraphic positions within the unit, and the measured thermal conductivities should be representative of the unit as a whole.

However, only four samples from Unit TSw1 were tested. It is unlikely that such a small sampling of the unit could represent the

entire variation in mineralogy expected for the unit. Examination of mineralogic data in Bish and Chipera (1989) for samples close to the four thermal-conductivity samples suggests that mineralogic variability in the four samples is quite large. Thus, the mean value and standard deviation for measured thermal conductivities of Unit TSw1 may not be significantly different than the values that would be obtained from a larger set of samples. This supposition is supported by the good agreement between the in situ thermal conductivities estimated for this report and the data from Sass et al. (1988).

4.0 CONCLUSIONS

Modeling of the saturation behavior of the thermal conductivity samples during experiments suggests that the behavior is quite different than that assumed previously. Samples may have saturations of 0.5 or greater at the end of an experiment. In addition, the distribution of pore water within a sample after dehydration begins appears to vary radially, so that the assumption that the material is homogeneous cannot be justified. These considerations have led to the decision not to use thermal-conductivity data gathered at temperatures above the nominal boiling temperature.

Also, a new empirical model was selected to calculate the thermal conductivities of multi-phase materials. A model described by Brailsford and Major (1964) is judged to be more applicable to the range of saturation conditions in the tuffaceous samples than is the geometric-mean model used in previous work. Combination of the new model with the measured thermal conductivities and with data on matrix porosity, lithophysal-cavity abundance, and fracture porosity has allowed estimation of in situ thermal conductivities for units TSw1 and TSw2. The estimated values are provided in Table 7.

There remain several areas for future work on the thermal conductivity of the welded, devitrified material. The porosities of the experiment samples should be determined in order to enable better estimates of K_o to be made. In addition, after making low-temperature measurements on the saturated samples, the samples should be oven-dried to completely

Table 7

Estimated Values of In Situ Thermal Conductivities
for the Welded, Devitrified Topopah Spring Member

	Thermal Conductivity (W/m-K)			
	In Situ Saturation[1]		Dry	
Thermal/Mechanical Unit	Mean Value	St. Dev.	Mean Value	St. Dev.
TSw1 - Average	1.7	0.3	1.6	0.3
Lithophysae-Rich	1.6	0.2	1.5	0.2
TSw2 - Average	2.1	0.2	2.1	0.2

1: "In situ saturation" has been assumed to be 0.65±0.19 in the matrix porosity, with lithophysal cavities and fractures assumed to be dry.

remove the pore water and a series of thermal-conductivity measurements should be made at all temperatures of interest. These measurements will assist in verifying the tentative conclusion made in this document that K_o is not temperature-dependent, and will provide reliable data for estimation of in situ thermal conductivities at high temperatures.

One final area of investigation should be measurement of the thermal conductivity of partially saturated samples. Pratt (1969) suggests the possibility that, because of latent-heat effects, partial saturation may result in higher thermal conductivities than those measured at full saturation. If this possibility turns out to be true, the data given in Table 7 would not be bounding values on the in situ thermal conductivity of the welded, devitrified tuffs.

5.0 REFERENCES

Abernethy, R. B., R. P. Benedict, and R. B. Dowdell, 1985. ASME Measurement Uncertainty; J. Fluids Engineering, Vol. 107, pp. 161-164 (NNA.891222.0025).

Bish, D. L., and S. J. Chipera, 1989. Revised Mineralogic Summary of Yucca Mountain, Nevada; LA-11497-MS, Los Alamos National Laboratory, Los Alamos, NM (NNA.891019.0029).

Brailsford, A. D., and K. G. Major, 1964. The Thermal Conductivity of Aggregates of Several Phases, Including Porous Materials; Brit. Jour. Appl. Phys., Vol. 15, pp. 313-319 (NNA.890522.0278).

DOE (U.S. Department of Energy), 1989. The Yucca Mountain Project Reference Information Base; Version 4, Nevada Operations Office, Las Vegas, Nevada, February 1989 (NNA.890330.0077).

Hadley, G. R., 1985. PETROS -- A Program for Calculating Transport of Heat, Water, Water Vapor, and Air Through a Porous Material; SAND84-0878, Sandia National Laboratories, Albuquerque, NM (NN1.881007.0038).

Kestin, J., 1978. Thermal Conductivity of Water and Steam; Mech. Eng. Vol. 100, pp. 46-48 (NNA.890713.0187).

Klavetter, E. A., and R. R. Peters, 1986. Estimation of Hydrologic Properties of An Unsaturated, Fractured Rock Mass; SAND84-2642, Sandia National Laboratories, Albuquerque, NM (NNA.870317.0738).

Klavetter, E. A., and R. R. Peters, 1987. An Evalution of the Use of Mercury Porosimetry in Calculating Hydrologic Properties of Tuffs From Yucca Mountain, Nevada; SAND86-0286, Sandia National Laboratories, Albuquerque, NM (NNA.890327.0056).

Lappin, A. R., 1980. Thermal Conductivity of Silicic Tuffs: Predictive Formalism and Comparison With Preliminary Experimental Results; SAND80-0769, Sandia National Laboratories, Albuquerque, NM (HQS.880517.1665).

Lappin, A. R., and F. B. Nimick, 1985a. Bulk and Thermal Properties of the Functional Tuffaceous Beds in Holes USW G-1, UE-25a#1, and USW G-2, Yucca Mountain, Nevada; SAND82-1434, Sandia National Laboratories, Albuquerque, NM (HQS.880517.1666).

Lappin, A. R., and F. B. Nimick, 1985b. Thermal Properties of the Grouse Canyon Member of the Belted Range Tuff and of Tunnel Bed 5, G-Tunnel, Nevada Test Site; SAND82-2203, Sandia National Laboratories, Albuquerque, NM (HQS.880517.1667).

Lappin, A. R., R. G. Van Buskirk, D. O. Enniss, S. W. Butters, F. M. Prater, C. S. Muller, and J. L. Bergosh, 1982. Thermal Conductivity, Bulk Properties, and Thermal Stratigraphy of Silicic Tuffs from the Upper Portion of Hole USW-G1, Yucca Mountain, Nye County, Nevada; SAND81-1873, Sandia National Laboratories, Albuquerque, NM (NNA.870406.0071).

Montazer, P., and W. E. Wilson, 1984. Conceptual Hydrologic Model of Flow in the Unsaturated Zone, Yucca Mountain, Nevada; USGS-WRIR-84-4345, U.S. Geological Survey, Denver, CO (HQS.880517.1675).

Nimick, F. B., 1989. Thermal-Conductivity Data for Tuffs From the Unsaturated Zone at Yucca Mountain, Nevada; SAND88-0624, Sandia National Laboratories, Albuquerque, NM (NNA.890515.0133).

Nimick, F. B., and A. R. Lappin, 1985. Thermal Conductivity of Silicic Tuffs from Yucca Mountain and Rainier Mesa, Nye County, Nevada; SAND83-1711J, Sandia National Laboratories, Albuquerque, NM (HQS.880517.1684).

Nimick, F. B., and B. M. Schwartz, 1987. Bulk, Thermal, and Mechanical Properties of the Topopah Spring Member of the Paintbrush Tuff, Yucca Mountain, Nevada; SAND85-0762, Sandia National Laboratories, Albuquerque, NM (SRX.871014.6257).

Peters, R. R., E. A. Klavetter, I. J. Hall, S. C. Blair, P. R. Heller, and G. W. Gee, 1984. Fracture and Matrix Hydrologic Characteristics of Tuffaceous Materials from Yucca Mountain, Nye County, Nevada; SAND84-1471, Sandia National Laboratories, Albuquerque, NM (NNA.870407.0036).

Pratt, A. W., 1969. Heat Transmission in Low Conductivity Materials; in Tye, R. P. (ed.), Thermal Conductivity; Academic Press (New York), pp. 301-405 (NNA.891106.0191).

Sass, J. H., A. H. Lachenbruch, W. W. Dudley, Jr., S. S. Priest and R. J. Monroe, 1988. Temperature, Thermal Conductivity, and Heat Flow Near Yucca Mountain, Nevada: Some Tectonic and Hydrologic Implications; USGS-OFR-87-649, U. S. Geological Survey, Denver, CO (NNA.890123.0010).

Tillerson, J. R., and F. B. Nimick (eds.), 1984. Geoengineering Properties of Potential Repository Units at Yucca Mountain, Southern Nevada; SAND84-0221, Sandia National Laboratories, Albuquerque, NM (NNA.870406.0308).

Woodside, W., and J. H. Messmer, 1961. Thermal Conductivity of Porous Media. I. Unconsolidated Sands; Jour. Appl. Phys., Vol. 32, No. 9, pp. 1688-1699 (NNA.890515.0160).

Zimmerman, R. M., R. L. Schuch, D. S. Mason, M. L. Wilson, M. E. Hall, M. P. Board, R. P. Bellman, and M. L. Blanford, 1986a. Final Report: G-Tunnel Heated Block Experiment; SAND84-2620, Sandia National Laboratories, Albuquerque, NM (HQS.880517.1724).

Zimmerman, R. M., M. L. Blanford, J. F. Holland, R. L. Schuch, and W. H. Barrett, 1986b. Final Report: G-Tunnel Small-Diameter Heater Experiments; SAND84-2621, Sandia National Laboratories, Albuquerque, NM (HQS.880517.2365).

APPENDIX A

Propagation of Uncertainty During Calculations

Abernethy et al. (1985) outline a standard method of combining precisions or accuracies in measured parameters (e.g. temperature, length) to estimate the precision or accuracy of a property (e.g., thermal conductivity) calculated from the parameters. Assume that a property r is a function of several parameters P_j. Then the precision (S_r) and the accuracy (A_r) of r can be estimated using the following equations:

$$S_r = \left[\sum_{i=1}^{j} \left(\frac{\partial r}{\partial P_i} S_{P_i} \right)^2 \right]^{1/2} \qquad \text{(A-1)}$$

and

$$A_r = \left[\sum_{i=1}^{j} \left(\frac{\partial r}{\partial P_i} A_{P_i} \right)^2 \right]^{1/2}, \qquad \text{(A-2)}$$

where S_{P_i} and A_{P_i} are the precision and accuracy, respectively, associated with measurement of the parameter P_i and the partial derivatives are evaluated at the measured values of the P_i.

This method also is applicable to propagation of uncertainty (in the form of standard deviations in this report) associated with one or more properties through an equation to obtain the uncertainty associated with a calculated property. The generalized equation used to propagate uncertainties for this report is the following:

$$\sigma_{P_{calc}} = \left[\sum_{i=1}^{j} \left(\frac{\partial P_{calc}}{\partial P_i} \sigma_{P_i} \right)^2 \right]^{1/2} , \qquad \text{(A-3)}$$

where P_{calc} is the property to be calculated and σ represents standard deviation. For example, Equation 7 in Section 3.1 expresses K_o as a function of K, K_f, and ϕ. The uncertainty (standard deviation, σ) for K_o is calculated using:

$$\sigma_{K_o} = \left[\left(\frac{\partial K_o}{\partial K} \sigma_k \right)^2 + \left(\frac{\partial K_o}{\partial \phi} \sigma_\phi \right)^2 \right]^{1/2} , \qquad \text{(A-4)}$$

where σ_K and σ_ϕ are the standard deviations for measured thermal conductivity and matrix porosity, respectively. (Normally, σ_{K_f} would also appear in the equation, but in this case $\sigma_{K_f} = 0$ because published values for the thermal conductivity of water are used in calculating K_o.)

This method of uncertainty propagation assumes that the function representing P_{calc} is approximately linear over the range $P_{calc} \pm \sigma_{P_{calc}}$. The validity of the assumpton of linearity was checked for each uncertainty propagation performed for this report. Checks were made for the following cases:

- Calculation of K_f from data on s, K_w and K_a;
- Calculation of K_o from data on K_f, ϕ, and measured thermal conductivity;

- Calculation of in situ thermal conductivity of nonlithophysal material from data on K_o, ϕ and K_f; and
- Calculation of in situ thermal conductivity for lithophysal material from data on in situ thermal conductivity of nonlithophysal material, K_f and lithophysal porosity.

As appropriate, each of the four cases above was subdivided to perform equivalent calculations at different temperatures for each of the two thermal/mechanical Units TSw1 and TSw2.

In all, 65 calculations were performed to examine the assumption of linearity. The departure from linearity, δ, is expressed as

$$\delta = |\text{ line - function}|/\text{line}. \qquad \text{(A-5)}$$

Out of the 65 calculations, only four showed maximum values of δ greater than 0.002. These four all were calculations for K_f as a function of in situ saturation at different temperatures. The maximum value of δ for each case was approximately 0.057, obtained at the minimum in situ saturation of 0.46.

In some cases, such large deviations from linearity might present a problem. However, the calculated standard deviations for K_f (Table 5 in the main text) are approximately 48% of the mean values, or a factor of eight larger than the "error" introduced by assuming linearity for uncertainty propagation. Thus, the conclusion is made that the assumption of linearity is reasonable for this study.

APPENDIX B

Applicability to Reference Information Base and Site and Engineering Property Data Base

Data presented in Table 7 are intended for submittal to the Reference Information Base (RIB) (DOE, 1989). Saturation data for the welded portion of the Topopah Spring Member have been referenced to Montazer and Wilson (1984); the same values are listed in Section 1.4.2 (Revision 0) of Version 4 of the RIB. Data for matrix porosity and lithophysal-cavity abundance have been referenced to Nimick and Schwartz (1987); equivalent data in the RIB are too generic to be used in the interpretation of sample-specific thermal conductivity data.

No data in this document are intended for entry into the Site and Engineering Property Data Base.

DISTRIBUTION LIST

Samuel Rousso, Acting Director (RW-1)
Office of Civilian Radioactive
Waste Management
U.S. Department of Energy
Forrestal Bldg.
Washington, D.C. 20585

Ralph Stein (RW-30)
Office of Civilian Radioactive
Waste Management
U.S. Department of Energy
Forrestal Bldg.
Washington, D.C. 20585

M. W. Frei (RW-22)
Office of Civilian Radioactive
Waste Management
U.S. Department of Energy
Forrestal Bldg.
Washington, D.C. 20585

B. G. Gale (RW-23)
Office of Civilian Radioactive
Waste Management
U.S. Department of Energy
Forrestal Bldg.
Washington, D.C. 20585

F. G. Peters (RW-2)
Office of Civilian Radioactive
Waste Management
U.S. Department of Energy
Forrestal Bldg.
Washington, D.C. 20585

J. D. Saltzman (RW-20)
Office of Civilian Radioactive
Waste Management
U.S. Department of Energy
Forrestal Bldg.
Washington, D.C. 20585

S. J. Brocoum (RW-221)
Office of Civilian Radioactive
Waste Management
U.S. Department of Energy
Forrestal Building
Washington, D.C. 20585

T. H. Isaacs (RW-40)
Office of Civilian Radioactive
Waste Management
U.S. Department of Energy
Forrestal Bldg.
Washington, D.C. 20585

D. H. Alexander (RW-332)
Office of Civilian Radioactive
Waste Management
U.S. Department of Energy
Forrestal Bldg.
Washington, D.C. 20585

J. C. Bresee (RW-10)
Office of Civilian Radioactive
Waste Management
U.S. Department of Energy
Forrestal Bldg.
Washington, D.C. 20585

Gerald Parker (RW-333)
Office of Civilian Radioactive
Waste Management
U.S. Department of Energy
Forrestal Bldg.
Washington, D.C. 20585

Senior Project Manager for Yucca
Mountain
Repository Project Branch
Division of Waste Management
U.S. Nuclear Regulatory Commission
Washington, D.C. 20555

NTS Section Leader
Repository Project Branch
Division of Waste Management
U.S. Nuclear Regulatory Commission
Washington, D.C. 20555

Repository Licensing & Quality
Assurance
Project Directorate
Division of Waste Management
U.S. Nuclear Regulatory Commission
Washington, DC 20555

NRC Document Control Clerk
Division of Waste Management
U.S. Nuclear Regulatory Commission
Washington, D.C. 20555

Carl P. Gertz, Project Manager (5)
Yucca Mountain Project Office
Nevada Operations Office
U.S. Department of Energy
Mail Stop 523
P.O. Box 98518
Las Vegas, NV 89193-8518

T. H. Beall (12)
Technical Information office
Nevada Operations Office
U. S. Department of Energy
P.O. Box 98518
Las Vegas, NV 89193-8518

C. L. West, Director
Office of External Affairs
U.S. Department of Energy
Nevada Operations Office
P.O. Box 98518
Las Vegas, NV 89193-8518

W. M. Hewitt, Program Manager
Roy F. Weston, Inc.
955 L'Enfant Plaza, Southwest
Suite 800
Washington, D.C. 20024

Technical Information Center
Roy F. Weston, Inc.
955 L'Enfant Plaza, Southwest
Suite 800
Washington, D.C. 20024

L. J. Jardine (15)
Actg. Technical Project Officer for YMP
Lawrence Livermore National Laboratory
Mail Stop L-204
P.O. Box 808
Livermore, CA 94550

J. H. Nelson
Technical Project Officer for YMP
Science Applications International Corp.
101 Convention Center Dr.
Suite 407
Las Vegas, NV 89109

H. N. Kalia
Exploratory Shaft Test Manager
Los Alamos National Laboratory
Mail Stop 527
101 Convention Center Dr.
Suite P230
Las Vegas, NV 89109

R. J. Herbst (40)
Technical Project Officer for YMP
Los Alamos National Laboratory
N-5, Mail Stop J521
P.O. Box 1663
Los Alamos, NM 87545

L. R. Hayes (6)
Technical Project Officer for YMP
U.S. Geological Survey
P.O. Box 25046
421 Federal Center
Denver, CO 80225

K. W. Causseaux
NHP Reports Chief
U.S. Geological Survey
P.O. Box 25046
421 Federal Center
Denver, CO 80225

R. V. Watkins, Chief
Project Planning and Management
U.S. Geological Survey
P.O. Box 25046
421 Federal Center
Denver, CO 80225

Center for Nuclear Waste Regulatory Analyses
6220 Culebra Road
Drawer 28510
San Antonio, TX 78284

D. L. Lockwood, General Manager
Las Vegas Branch
Fenix & Scisson, Inc.
Mail Stop 514
P.O. Box 93265
Las Vegas, NV 89193-3265

R. L. Bullock
Technical Project Officer for YMP
Fenix & Scisson, Inc.
Mail Stop 403
101 Convention Center Dr.
Suite P250
Las Vegas, NV 89193-3265

James C. Calovini
Technical Project Officer for YMP
Holmes & Narver, Inc.
101 Convention Center Dr.
Suite 860
Las Vegas, NV 89109

Dr. David W. Harris
YMP Technical Project Officer
Bureau of Reclamation
P.O. Box 25007 Bldg. 67
Denver Federal Center
Denver, CO 80225-0007

M. D. Voegele
Science Applications International Corp.
101 Convention Center Dr.
Suite 407
Las Vegas, NV 89109

J. A. Cross, Manager
Las Vegas Branch
Fenix & Scisson, Inc.
P.O. Box 93265
Mail Stop 514
Las Vegas, NV 89193-3265

P. T. Prestholt
NRC Site Representative
1050 East Flamingo Road
Suite 319
Las Vegas, NV 89119

A. E. Gurrola, General Manager
Energy Support Division
Holmes & Narver, Inc.
P.O. Box 93838
Mail Stop 580
Las Vegas, NV 89193-3838

R. E. Lowder
Technical Project Officer for YMP
MAC Technical Services
Valley Bank Center
101 Convention Center Drive
Suite P-113
Las Vegas, NV 89109

B. L. Fraser, General Manager
Reynolds Electrical & Engineering Co.
P.O. Box 98521
Mail Stop 555
Las Vegas, NV 89193-8521

P. K. Fitzsimmons, Director
Health Physics & Environmental Division
Nevada Operations Office
U.S. Department of Energy
P.O. Box 98518
Las Vegas, NV 89193-8518

Robert F. Pritchett
Technical Project Officer for YMP
Reynolds Electrical & Engineering Co.
Mail Stop 615
P.O. Box 98521
Las Vegas, NV 89193-8521

Elaine Ezra
YMP GIS Project Manager
EG&G Energy Measurements, Inc.
P.O. Box 1912
Mail Stop H-02
Las Vegas, NV 89125

SAIC-T&MSS Library (2)
Science Applications International Corp.
101 Convention Center Dr.
Suite 407
Las Vegas, NV 89109

Dr. Martin Mifflin
Desert Research Institute
Water Resources Center
2505 Chandler Avenue
Suite 1
Las Vegas, NV 89120

E. P. Binnall
Field Systems Group Leader
Building 50B/4235
Lawrence Berkeley Laboratory
Berkeley, CA 94720

J. F. Divine
Assistant Director for
Engineering Geology
U.S. Geological Survey
106 National Center
12201 Sunrise Valley Dr.
Reston, VA 22092

V. M. Glanzman
U.S. Geological Survey
P.O. Box 25046
913 Federal Center
Denver, CO 80225

C. H. Johnson
Technical Program Manager
Nuclear Waste Project Office
State of Nevada
Evergreen Center, Suite 252
1802 North Carson Street
Carson City, NV 89710

T. Hay, Executive Assistant
Office of the Governor
State of Nevada
Capitol Complex
Carson City, NV 89710

R. R. Loux, Jr., (3)
Executive Director
Nuclear Waste Project Office
State of Nevada
Evergreen Center, Suite 252
1802 North Carson Street
Carson City, NV 89710

John Fordham
Desert Research Institute
Water Resources Center
P.O. Box 60220
Reno, NV 89506

Prof. S. W. Dickson
Department of Geological Sciences
Mackay School of Mines
University of Nevada
Reno, NV 89557

J. R. Rollo
Deputy Assistant Director for
Engineering Geology
U.S. Geological Survey
106 National Center
12201 Sunrise Valley Dr.
Reston, VA 22092

Eric Anderson
Mountain West Research-Southwest
Inc.
Phoenix Gateway Center
432 North 44 Street
Suite 400
Phoenix, AZ 85008-6572

Judy Foremaster (5)
City of Caliente
P.O. Box 158
Caliente, NV 89008

D. J. Bales
Science and Technology Division
Office of Scientific and Technical
Information
U.S. Department of Energy
P.O. Box 62
Oak Ridge, TN 37831

Carlos G. Bell, Jr.
Professor of Civil Engineering
Civil and Mechanical Engineering
Department
University of Nevada, Las Vegas
4505 South Maryland Parkway
Las Vegas, NV 89154

C. F. Costa, Director
Nuclear Radiation Assessment
Division
U.S. Environmental Protection
Agency
Environmental Monitoring Systems
Laboratory
P.O. Box 93478
Las Vegas, NV 89193-3478

J. Z. Bem
Project Manager
Bechtel National Inc.
P.O. Box 3965
San Francisco, CA 94119

R. Harig
Parsons Brinckerhoff Quade &
Douglas
1625 Van Ness Ave.
San Francisco, CA 94109-3679

Dr. Roger Kasperson
CENTED
Clark University
950 Main Street
Worcester, MA 01610

Robert E. Cummings
Engineers International, Inc.
P.O. Box 43817
Tucson, AZ 85733-3817

Dr. Jaak Daemen
Department of Mining and
Geotechnical Engineering
University of Arizona
Tucson, AZ 85721

Department of Comprehensive Planning
Clark County
225 Bridger Avenue, 7th Floor
Las Vegas, NV 89155

Economic Development Department
City of Las Vegas
400 East Stewart Avenue
Las Vegas, NV 89109

Planning Department
Nye County
P.O. Box 153
Tonopah, NV 89049

Director of Community Planning
City of Boulder City
P.O. Box 367
Boulder City, NV 89005

Commission of the European
Communities
200 Rue de la Loi
B-1049 Brussels
Belgium

Lincoln County Commission
Lincoln County
P.O. Box 90
Pioche, NV 89043

Community Planning & Development
City of North Las Vegas
P.O. Box 4086
North Las Vegas, NV 89030

City Manager
City of Henderson
Henderson, NV 89015

ONWI Library
Battelle Columbus Laboratory
Office of Nuclear Waste Isolation
505 King Avenue
Columbus, OH 43201

Librarian
Los Alamos Technical
Associates, Inc.
P.O. Box 410
Los Alamos, NM 87544

Loren Lorig
Itasca Consulting Group, Inc.
1313 5th Street SE, Suite 210
Minneapolis, MN 55414

Edward Kansa
MS L-200
Lawrence Livermore National
Laboratory
P.O. Box 808
Livermore, CA 94550

John Sass
U. S. Geological Survey
2255 N. Gemini Dr.
Flagstaff, AZ 86001

James K. Lein
Dept. of Geography
122 Clippinger Laboratories
Ohio University
Athens, OH 45701-2979

6300 R. W. Lynch
6310 T. O. Hunter
6310A F. W. Bingham
6310 YMPCRF
6310 100/124213/SAND86-0090/NQ
6311 A. L. Stevens
6311 R. E. Finley
6312 J. C. Cummings
6313 T. E. Blejwas
6314 L. S. Costin
6314 S. J. Bauer
6314 F. D. Hansen
6314 E. E. Ryder
6315 L. E. Shephard
6315 A. C. Davis (2)
for DRMS Data Sets
51/L01A-6/24/80
51/L01A-7/16/81
51/L01A-10/7/81
51/L01A-9/7/82
51/L01A-12/2/82
6315 F. B. Nimick (5)
6315 R. H. Price
6316 R. P. Sandoval
6317 S. Sinnock
6318 T. O. Hunter, Actg.
6318 C. Mora (2)
6318 D. Shaw
for Accession No. Data Base
6319 T. O. Hunter, Actg.
6332 WMT Library (20)
6410 D. J. McCloskey, Actg.
3141 S. A. Landenberger (5)
3151 W. I. Klein (3)
8524 J. A. Wackerly
3154-1 C. L. Ward (8)
for DOE/OSTI

THE NUMBER IN THE LOWER-RIGHT-HAND CORNER IS AN ACCESSION NUMBER USED FOR OCRWM RECORDS MANAGEMENT PURPOSES ONLY. IT SHOULD NOT BE USED WHEN ORDERING THIS PUBLICATION.

Org.	Bldg.	Name	Rec'd by	Org.	Bldg.	Name	Rec'd by

Sandia National Laboratories